Genomic and transcriptomic characterization of the Collimonas quorum sensing genes and regulon

Stephane Uroz, Océane Geisler, Laure Fauchery, Raphaël Lami, Alice M.S. Rodrigues, Emmanuelle Morin, Johan Leveau, Phil M. Oger

FEMS Microbiology Ecology, 2022, 98, 1–22
DOI: 10.1093/femsec/fiac100
Advance access publication date: 30 August 2022
Research Article

Genomic and transcriptomic characterization of the *Collimonas* quorum sensing genes and regulon

Stephane Uroz[1,2,*], Océane Geisler[1], Laure Fauchery[1], Raphaël Lami[3], Alice M. S. Rodrigues[3], Emmanuelle Morin[1], Johan H. J. Leveau[4], Philippe Oger[5]

[1]Université de Lorraine, INRAE, UMR1136 "Interactions Arbres-Microorganismes", F-54280 Champenoux, France
[2]INRAE, UR1138 "Biogéochimie des écosystèmes forestiers", F-54280 Champenoux, France
[3]Sorbonne Université, CNRS, Laboratoire de Biodiversité et Biotechnologies Microbiennes (LBBM, USR3579), Fédération de Recherche FR3724, Observatoire Océanologique, 66650 Banyuls-sur-Mer, France
[4]Department of Plant Pathology, University of California - Davis, Davis, CA 95616, United States
[5]Université Lyon, INSA de Lyon, CNRS UMR 5240, F-69622 Villeurbanne, France
*Corresponding author: Université de Lorraine, INRAE, "Interactions Arbres Microorganismes", UMR 1136, 54280 Champenoux, France. Tel: +33 (0)383394081; Fax: +33 (0)383394069; E-mail: stephane.uroz@inrae.fr
Editor: Paolina Garbeva

Abstract

Collimonads are well-adapted to nutrient-poor environments. They are known to hydrolyse chitin, produce antifungal metabolites, weather minerals, and are effective biocontrol agents protecting plants from fungal diseases. The production of *N*-acyl homoserine lactones (AHLs) was suggested to be a conserved trait of collimonads, but little is known about the genes that underlie this production or the genes that are controlled by AHLs. To improve our understanding of the role of AHLs in the ecology of collimonads, we carried out transcriptomic analyses, combined with chemical and functional assays, on strain *Collimonas pratensis* PMB3(1). The main AHLs produced by this strain were identified as 3-hydroxy-hexa- and octa-noyl-homoserine lactone. Genome analysis permitted to identify putative genes coding for the autoinducer synthase (*colI*) and cognate transcriptional regulator (*colR*). The ability to produce AHLs was lost in Δ*colI* and Δ*colR* mutants. Functional assays revealed that the two mutants metabolized glucose, formate, oxalate, and leucine better than the wild-type (WT) strain. Transcriptome sequencing analyses revealed an up-regulation of different metabolic pathways and of motility in the QS-mutants compared to the WT strain. Overall, our results provide insights into the role of the AHL-dependent regulation system of *Collimonas* in environment colonization, metabolism readjustment, and microbial interactions.

Keywords: acyl homoserine lactone, *Collimonas*, mycorrhizosphere, transcriptomics

Introduction

Quorum sensing (QS) is a widespread regulatory mechanism used by bacteria to regulate and coordinate gene expression in a cell-density dependent manner (Whitehead et al. 2001, Mukherjee and Bassler 2019). QS relies on the production and perception of specific signal molecules by cells in the bacterial population (Whitehead et al. 2001, Sperandio 2010, Papenfort and Bassler 2016). The most common and most studied QS signal molecules found in Gram-negative bacteria are *N*-acyl-L-homoserine lactones (AHL; Whitehead et al. 2001), whereas Gram-positive bacteria mostly use small peptides (Kleerebezem et al. 1997). AHLs exhibit a conserved structure, with a homoserine lactone (HSL) ring, i.e. *N*-linked to an acyl chain ranging from 4 to 18 carbons in length. The length of the acyl chain and the oxidation status of the C3 position of the acyl chain provide for specificity of the QS signal (Fuqua et al. 2001). AHLs are produced through a LuxI-like synthase and perceived by a LuxR-type sensor, which acts as a transcriptonal regulator and binds to a specific sequence in the promoter region of the gene(s) whose transcription is AHL-controlled (Fuqua et al. 1994). Synchronization of gene expression occurs when a threshold concentration of AHLs is reached, allowing the induction or repression of gene expression. A broad range of biological functions have been shown to be regulated through QS systems in bacteria, such as antibiotic and enzyme production, motility, biofilm formation, conjugation, and symbiosis (Winson et al. 1995, Wood et al. 1997, Whitehead et al. 2002, Wisniewski-Dyé and Downie 2002, Brennan et al. 2013). Recent findings also suggest that QS is involved in the regulation of primary metabolism (LaRock et al. 2013, Goo et al. 2015, Carneiro et al. 2020). For example, regulation of glucose, glyoxylate, or oxalate metabolic pathways through an AHL-dependent system has been reported for different *Burkholderia* species (Goo et al. 2015; An et al. 2014). While the QS regulation system has been largely investigated in pathogenic bacteria (Swift et al. 2001, Whitehead et al. 2001, Mukherjee and Bassler 2019, LaRock et al. 2013), it can also be found in beneficial bacteria such as plant growth-promoting rhizobacteria and biocontrol agents (Wood et al. 1997, Zúñiga et al. 2013; Rankl et al. 2016).

A wide range of Gram-negative taxa have been shown to produce AHLs, including representatives of the α-, β, and γ-Proteobacteria or Bacteroidetes (Gray and Garey 2001, Romero et al. 2010). The AHLs produced can strongly differ from one strain to another strain and the use of LC-MS/MS highlighted that the variety of AHL produced by one strain can be very high (Ortori et al. 2007, Rasmussen et al. 2014, Patel et al. 2016). In the soil environment, and more particularly in the close vicinity of the roots where competition for nutritive resources is fierce, AHL-

Received: May 22, 2022. **Revised:** July 13, 2022. **Accepted:** August 26, 2022

producing bacteria can represent 10%–40% of the culturable population (Steidle et al. 2001, Dangelo-Picard et al. 2005, Schaefer et al. 2013). While this ability was largely investigated in the rhizosphere and in the context of the production of antifungal metabolites (i.e. phenazine; Pierson and Pierson 1996), few studies have considered the role of AHLs in the mycorrhizosphere (i.e. plant roots colonized by a symbiotic fungus; Rambelli 1973, Johansson et al. 2004). The mycorrhizosphere represents a distinct environment compared to the rhizosphere, both physically and chemically, as it relies on the establishment and functioning of a symbiotic interaction between plant roots and mycorrhizal fungi. This symbiosis strongly modifies soil properties, but also plant functioning, which in turn impacts the associated microbial communities (Johansson et al. 2004, Marupakula et al. 2017, Uroz et al. 2019, 2012, Pratama and van Elsas 2019). Several studies have shown that both the taxonomic and functional structures of the mycorrhizosphere-associated microbiota changed compared to the surrounding bulk soil (Viollet et al. 2011, Uroz et al. 2007). In addition, different bacterial communities can be selected on different fine roots of the same root system depending on the fungal partner present (Uroz et al. 2012, Marupakula et al. 2017). Noticeably, the mycorrhizosphere appeared enriched in bacteria capable of metabolizing fungal metabolites (i.e. trehalose, Frey-Klett et al. 2005), hydrolysing chitin (Uroz et al. 2013), affecting fungal development (Deveau et al. 2007), and weathering minerals (Uroz et al. 2007). All these findings support essential interactions and signaling between symbiotic fungi and bacterial communities (Bonfante and Anca 2009, Frey-Klett et al. 2011, Venturi and Keel 2016, Pratama and van Elsas 2019). However, our knowledge about the ability of mycorrhizospheric bacteria to produce QS signal molecules and about the functions that these molecules regulate remains limited, as does our understanding of the direct role of such signals on the plant-symbiotic fungi. AHL-producing bacteria have been recovered from spores of *Rhizophagus intraradices* (Palla et al. 2018) and different fungi isolated from tree root system have been reported for their ability to perturb AHL-based communication (Rasmussen et al. 2005, Uroz and Heinonsalo 2008), suggesting a role of these signal molecules in bacteria–fungi interactions. Culturable representatives of the *Sinorhizobium* and *Collimonas* coming from the mycorrhizosphere have been reported for their ability to produce AHLs (Leveau et al. 2010, Song et al. 2015, Palla et al. 2018).

Collimonads belong to the *Oxalobacteraceae* family, which is well known for the antifungal activities of its members (*Collimonas*, *Duganella*, and *Janthinobacterium*; de Boer et al. 2005, Haack et al. 2016). To date, six *Collimonas* species (*C. fungivorans*, *C. pratensis*, *C. arenae*, *C. anthrihumi*, *C. silvisoli*, and *C. humicola*) have been described (de Boer et al. 2004, Höppener-Ogawa et al. 2008, Lee 2018, Li et al. 2021). Combination of culture-dependent and -independent analyses revealed that collimonads are relatively rare in the bulk soil (Lepleux et al. 2012, Uroz et al. 2012, Cretoiu et al. 2013), but abundantly represented in specific habitats such as the mycorrhizosphere (Uroz et al. 2012) and mineralosphere (Lepleux et al. 2012, Colin et al. 2017). Initially studied due to their ability to grow at the expense of living fungal hyphae (mycophagy), collimonads are now also known to hydrolyze chitin (de Boer et al. 1998, 2001, 2005, Fritsche et al. 2008, Leveau and Preston 2008, Senechkin et al. 2013, Ballhausen et al. 2016), produce antifungal metabolites (i.e. collimomycins; Fritsche et al. 2014; carenaemin; Akum et al. 2021), weather minerals (Uroz et al. 2009), and act as effective biocontrol agents (Kamilova et al. 2007, Doan et al. 2020). The activation of many of these functions in presence of fungi (Mela et al. 2011, Haack et al. 2016) suggests a specialization in obtaining nutrients from fungal origin and strong interactions with the soil mycobiota.

In this study, we identified and characterized the AHL-dependent QS regulon, the AHL molecules produced as well as the QS-regulated genes in *C. pratensis* strain PMB3(1), which is a model bacterial strain for the study of mineral weathering in the mycorrhizosphere (Uroz et al. 2014, Picard et al. 2021). To this extent, we used chromatography, genomic and transcriptomic analyses on strain PMB3(1). We found a strong sequence conservation of the AHL synthase and transcriptional regulator encoding genes among different *Collimonas* species, including strain PMB3(1). Using targeted and random mutagenesis approaches we confirmed the role of the luxI and luxR homologues. Through the comparison of the wild-type (WT) strain and QS mutants with RNA seq analyses, we uncovered the complex remodelling of *Collimonas* metabolism by AHLs as well as the regulation of various enzymatic activities with potential role in adaptation to the mycorrhizosphere.

Material and methods

Bacterial strains, plasmids, and culture media

Bacterial strain PMB3(1) was isolated from the oak/*Scleroderma citrinum* mycorrhizosphere (Calvaruso et al. 2007). It was chosen for this study because it is very effective at weathering mineral, hydrolyzing chitin, and inhibiting fungal growth. Its genome has been sequenced (Picard et al. 2020) and presents a good completeness (99.7%) according to a CheckM analysis (Parks et al. 2015). In addition, a set of other *Collimonas* strains with different ecological origin and from different species was cultivated in our study. All the bacterial strains and plasmids used in the present study are listed in Table 1. Strains of *Collimonas* and the bionsensor *Chromobacterium violaceum* CV026 were grown in low-salt lysogeny broth (LBm) medium at 25°C and 28°C, respectively; *Escherichia coli* strains were cultivated in LB medium at 37°C. The bionsensor *Agrobacterium tumefaciens* NTL4 was grown in AB medium (Chilton et al. 1974) at 28°C. The AB minimal (AB) medium was supplemented with mannitol (ABm; 2 g/l final concentration) as carbon source. Antibiotics, when required, were added to the media at the following final concentrations: Tetracycline 10 μg/ml, Kanamycin 100 μg/ml, Gentamycin 20 μg/ml, and Ampicillin 100 μg/ml. X-Gal (5-bromo-4-chloro-3-indolyl-β-D-galactopyranoside) was included in the medium at 40 μg/ml.

Chemicals and solvents

N-acyl-homoserine lactones (AHLs) were obtained from Cayman Chemical (Ann Arbor, MI, United States), Sigma-Aldrich or were kindly provided by Professor Paul Williams (University of Nottingham, UK). Stock solutions were obtained by dissolving standards in ethyl acetate, methanol or dichloromethane (C18-AHL) at a concentration of 1 mg/ml and stored at −80°C. Standard solutions for thin-layer chromatography (TLC) were prepared in ethyl acetate at the appropriate concentrations. Standard solutions for ultra performance liquid chromatography—high resolution mass spectrometry (UHPLC-HRMS/MS) analyses were prepared by diluting each individual standard solution with methanol in order to get a concentration range from 2000 to 20 ng/ml. The list of AHL standards used in UHPLC-HRMS/MS is provided in Table S1 (Supporting Information). LC-MS grade methanol, acetonitrile, and formic acid were purchased from Biosolve (Biosolve Chimie France, Dieuze), analytical-grade ethyl acetate was obtained from

Table 1. List of bacterial strains, plasmids, and constructions used in this study.

Strains	Characteristics	Reference
Collimonas pratensis PMB3(1)		Uroz et al. (2007)
Wild-type strain	Oak-*Scleroderma citrinum* mycorrhizosphere	
Δ*colR*	Tet^R, *colR*::pOT182 disruptant	This study
Δ*colI*	Gm^R, *colI*::Gm mutant	This study
Collimonas sp. PML3(2)	Oak-*Scleroderma citrinum* mycorrhizosphere	Uroz et al. (2007)
Collimonas sp. PML3(4)	Oak-*Scleroderma citrinum* mycorrhizosphere	Uroz et al. (2007)
Collimonas sp. PML3(8)	Oak-*Scleroderma citrinum* mycorrhizosphere	Uroz et al. (2007)
Collimonas sp. PMB2(3)	Oak-*Scleroderma citrinum* mycorrhizosphere	Uroz et al. (2007)
Collimonas pratensis Ter91	Coastal dune grassland	de Boer et al. (1998, 2004)
Collimonas fungivorans Ter331	Coastal dune grassland	de Boer et al. (1998, 2004)
Collimonas fungivorans Ter6	Coastal dune grassland	de Boer et al. (1998, 2004)
Collimonas pratensis Ter291	Coastal dune grassland	de Boer et al. (1998, 2004)
Collimonas arenae Ter282	Coastal dune grassland	de Boer et al. (1998, 2004)
Collimonas arenae Ter10	Coastal dune grassland	de Boer et al. (1998, 2004)
Collimonas arenae Cal35	Forest soil	Uroz et al. (2014)
Collimonas sp. Cal40	Forest soil	Uroz et al. (2014)
Collimonas sp. A41 (K1E3)	boreal oligotrophic forest soil/artic tundra	Männistö and Häggblom 2006)
Collimonas sp. A65 (K2E1)	boreal oligotrophic forest soil/artic tundra	Männistö and Häggblom (2006)
Collimonas sp. A133 (M1J3)	boreal oligotrophic forest soil/artic tundra	Männistö and Häggblom (2006)
Collimonas sp. A140 (M1R1)	boreal oligotrophic forest soil/artic tundra	Männistö and Häggblom (2006)
Collimonas sp. A206 (RA1BR1)	boreal oligotrophic forest soil/artic tundra	Männistö and Häggblom (2006)
Collimonas sp. A213 (RAJ3R1)	boreal oligotrophic forest soil/artic tundra	Männistö and Häggblom (2006)
Collimonas sp. A320 (S5T5)	boreal oligotrophic forest soil/artic tundra	Männistö and Häggblom (2006)
Escherichia coli		
DH5α	*supE44* Δ*lacU169* (Φ80*lacZ*ΔM15) *recA1 endA1 hsdR17 thi-1 gyrA96 relA1*	Lab collection
S17.1λpir	TpR Sm^R *recA thi pro hsdRM*$^+$ integrated RP4: 2-Tc:Mu: Km *Tn7* λ*pir*	Lab collection
Biosensors		
Agrobacterium tumefaciens NTL4(pZLR4)	Hydroxy, oxo, and long-chain AHL sensor strain	Luo et al. (2003)
Chromobacterium violaceum CV026	Reduced AHL sensor strain	McClean et al. (1997)
Plasmids		
pOT182	from pSUP102 (Gm^R) containing Tn5-OTl82 (Tet^R)	Dennis, and Zylstra (1998)
pUC1318::Gm	Amp^R Gm^R	Tichi and Tabita (2002)
pK19-mob	Km^R	Schäfer et al. (1994)
pGEM-T easy	Amp^R	Promega
pBBR-MCS2	Km^R	Kovach et al. (1995)
pG_ColI_PMB31	pGEM-T easy with the colI gene of strain PMB3(1)	This study
pG_ColI::Gm	pGEM-T easy with the colI gene of strain PMB3(1) with insertion of a Gm cassette at the SmaI site of colI	This study
pK_ColI::Gm	pK19-mob with a EcoRI fragment extracted from pG_ColI::Gm and containing colI::Gm	This study
pG_colI_Ter6	pGEM-T easy with the colI gene of strain Ter6	This study

Table 1. Continued

Strains	Characteristics	Reference
pG_colI_Ter10	pGEM-T easy with the colI gene of strain Ter10	This study
pG_colI_Ter331	pGEM-T easy with the colI gene of strain Ter331	This study
pG_colI_Ter282	pGEM-T easy with the colI gene of strain Ter282	This study
pG_colI_Ter91	pGEM-T easy with the colI gene of strain Ter91	This study
pG_colI_Ter291	pGEM-T easy with the colI gene of strain Ter291	This study
pG_colI_Cal35	pGEM-T easy with the colI gene of strain Cal35	This study
pB-colI	pBBR-MCS2 with a EcoRI/BamHI fragment containing the colI gene	This study
pB-colR	pBBR-MCS2 with a EcoRI/BamHI fragment containing the colR gene	This study

Sigma-Aldrich. Pure water was obtained from Elga Purelab Flex System (Veolia LabWater STI, Antony, France).

Detection and identification of the AHLs produced

The production of AHL was first evidenced in T streak assays (Steindler and Venturi 2007) using the *C. violaceum* CV026 biosensor. The different *Collimonas* strains, mutants or *E. coli* strains carrying the *luxI* homologue genes of the *Collimonas* strains in pGEM-T easy vector were streaked on LB medium as well as the *C. violaceum* CV026 biosensor. The production of violacein was scored after 2 and 4 days of incubation. For the thin layer chromatography (TLC) analyses, 10 ml of 2-days culture were extracted with equal volume of ethyl acetate and the extract was evaporated under vacuum and reconstituted in 100 µl of ethyl acetate. TLC was then used to separate and visualize the potential AHLs as described previously (Shaw et al. 1997). The TLC plates were then overlaid with the *C. violaceum* CV026 biosensor mixed with gelosed LB or with the *A. tumefaciens* NTL4(pZLR4) biosensor mixed with gelosed ABm.

For the UHPLC-HRMS/MS analyses, the extraction was done on 50 ml of 2-days culture (Doberva et al. 2017, Romani et al. 2021). In this case, the mixture of culture supernatant and ethyl acetate was shaken overnight at room temperature (150 r/m). The two phases were then separated and the aqueous phase was extracted once more. The two obtained organic phases were pooled and the solvent was evaporated under vacuum and reconstituted in 500 µl LCMS methanol. For the UHPLC-HRMS/MS analyses, a Q-Exactive Focus Orbitrap System coupled to an Ultimate 3000™ UHPLC system (Thermo Fisher Scientific) was used (Rodrigues et al. 2022). Analyses of extracts and standards (3 μl injected) were performed in electrospray positive ionization mode in the 50–750 m/z range in centroid mode. The parameters were as follows: spray voltage: 3 kV; sheath flow rate: 75; aux gas pressure: 20; capillary temperature: 350°C; heater temperature: 430°C. The analysis was conducted in FullMS data dependent MS2 mode (Discovery mode). Resolution was set to 70 000 in Full MS mode, and the AGC (automatic gain control) target was set to 1×10^6. In MS2 mode, resolution was 17 500, AGC target was set to 2×10^5, isolation window was 0.4 m/z, and normalized collision energy was stepped to 15, 30, and 40 eV. The UHPLC column was a Phenomenex Luna Omega Polar C18 1.6 μm, 150 × 2.1 mm. The column temperature was set to 42°C, and the flow rate was 0.4 ml/min. The solvent system was a mixture of water (A) with increasing proportions of acetonitrile (B), with both solvents modified with 0.1% formic acid. The gradient was as follows: 1% B 3 min before injection, then from 1 to 15 min, a gradient increase of B up to 100% (curve 5), followed by 100% B for 5 min. The flow was injected into the mass spectrometer starting immediately after injection. All data were acquired and processed using FreeStyle 1.5 software (Thermo Fisher Scientific). Standard solutions of each AHL were used to determine the limits of detection (LODs) and chromatographic retention times and to draw external calibration curves for AHL quantification (Rodrigues et al. 2022).

Tn5-pOT182 mutagenesis

In order to obtain QS mutants the WT strain PMB3(1) of *C. pratensis* was mutagenized with plasposon Tn5-pOT182 as described previously (Deshazer et al. 1997, Dennis et al. 1998), with minor modifications. The donor strain, *E. coli* S17-1λpir (pOT182), was grown at 37°C in antibiotic-containing LB broth overnight, and the recipient strain, *C. pratensis* PMB3(1), was grown at 25°C in ABm liquid medium for 2 days. On the day of the biparental conjugation, each culture (30 ml) was centrifuged and washed twice with sterile MQ water to remove any antibiotic from the medium and mixed in a final volume of 5 ml of sterile MQ water. The mixed suspension was spotted on agar LB plates (i.e. 10 µl drops). After 5 h of incubation at 25°C, the bacterial lawn of each plate was harvested using sterile MQ water (5 ml), and 150 µl of this suspension were plated on tetracycline-containing ABm plates for isolation of the Tn5 mutants of the strain PMB3(1). A total of 3000 mutants recovered after 5 days incubation at 25°C were organized in 96-well microplates. To confirm the presence of the plasposon in the genome of a set of randomly picked mutants, a portion of the plasposon sequence was amplified by PCR using pOT-For and pOT-Rev primers (Table 1).

Screening of the Tn5-pOT182 mutant library and other constructions

In order to screen the plasposon library for mutants affected in their ability to produce AHLs, square Petri dishes (120 × 120 mm) were poured with a mix (1:1) of gelosed LB and overnight liquid culture of *C. violaceum* CV026 grown in LB. A volume of 5 µl of liquid ABm liquid culture of each mutant of the library described

above was then spotted using a 96-well replicator on these indicatorplates. After 3-days culture, the presence/absence of purple pigment around the mutants was scored. All Tn5-pOT182 colonies lacking such purple pigment were tested independently a second time. All validated mutants were then used for molecular analyses and identification of any mutants affected including specifically Δ*colI* (i.e. AHL synthase) and Δ*colR* (i.e. LuxR-like transcriptional regulator) mutants.

Molecular methods

Total genomic DNA was extracted from the WT strain PMB3(1) and selected Tn5-pOT182 mutants using the protocol of Pospiech and Neumann (1995). For the Tn5-OT182 mutants, the flanking integration regions were identified using the rescue method as described previously (DeShazer et al. 1997). Briefly, 3 μg of DNA of each Tn5-OT182 mutant was digested overnight with *Eco*RI-HF in 50 μl. After heat inactivation, the digested DNA was ligated overnight in 20 μl and a volume of 10 μl was transformed into chemically competent *E. coli* DH5α. The transformants were recovered on gelosed AB mannitol medium. The resulting plasmids were extracted using the Miniprep kit from Qiagen and sequenced with the primer pOT-RT at Eurofins MWG Operon (https://www.eurofinsgenomics.eu/). All enzymes for restriction digestion and ligation were purchased from New England Biolabs and were used according to the manufacturers' instructions. When required, PCR amplicons were purified using QIAquick PCR purification and gel extraction kits from Qiagen. PCR reactions were performed using Taq polymerase from 5PRIME (Hamburg, Germany).

Construction of a *C. pratensis* PMB31 mutant affected in its AHL synthase

Because screening of the Tn5-pOT182 library did not yield mutants impacted in *colI*, a targeted knockout of this gene was generated. To do this, a *Sma*I restriction site was introduced in the AHL synthase encoding *colI* gene using a suite of three PCRs. The first PCR was done using the primer pair ColI-sens1: GCCAGT ACGCTCAGGCAAAG and ColI-RevSma1: TATGGCT⟨0:underline⟩ CCCGGG⟨/0:underline⟩TCGGCAG. The second PCR was done using ColI-sensSma2: CTGCCGA⟨0:underline⟩CCCGGG⟨/0:underline⟩AGCCATA and ColI-rev2 : AGTTGGTCACCCAGCAGGTAT. The third PCR was used using the primers ColI-sens1 and ColI-rev2 and the two previous PCR products as matrix. The final product was then extracted on 0.9% agarose gel and cloned in the pGEM-T-easy vector. The *colI* gene was then disrupted by insertion of a gentamicin resistance gene from pUC1318::Gm, cloned as an *Sma*I fragment at the unique *Sma*I site of the *colI* gene. The *colI*::Gm cassette was then cloned in the *Eco*RI site of the pK19-mob vector. The resulting construction was transferred in *E. coli* S17-1 λ-pyr and introduced by biparental conjugation in strain PMB3(1). The resulting colonies were then screened by PCR to identify double crossing-over mutants, which were tested for their ability to produce AHLs using the biosensors.

Complementation of the colI and colR mutant

To generate a construct for *colI* and *colR* gene complementation, primers were designed to be able to generate an *Eco*RI/*Bam*HI fragment containing the *colI* gene (TCGTGAAG⟨0:underline⟩GAATTC ⟨/0:underline⟩AGCGATGAAAG and AGGAT⟨0:underline⟩GAATCC ⟨/0:underline⟩GCCATGTGTC) and an *Eco*RI/*Bam*HI fragment containing the *colR* gene (TACGG⟨0:underline⟩GAATTC⟨/0:underline⟩AGGTATGGTTGAT and ACAGTTGCGC⟨0:underline⟩GGATCC⟨/0:underline⟩GCAATT). After amplification and purification, the resultant construct was cloned in PGEM-T easy and then excised by restriction enzyme cleavage and ligated with cleaved pBBR-MCS2 (*Eco*RI/*Bam*HI). The constructed plasmids were then transferred by conjugation from *E. coli* S17-1 λpir to the mutant strains of PMB3(1) Δ*colI* and Δ*colR* as described above, and then plated on ABm agar containing kanamycin (100 μg/ml) and tetracycline (10 μg/ml) or gentamycin (20 μg/ml), respectively for complementation of the Δ*colR* and Δ*colI* mutants. The ability to produce AHLs of the ΔcolI and ΔcolR mutants and their complemented versions (i.e. ΔcolI(pBBR-MCS2+colI) and ΔcolR (pBBR-MCS2+colR)) was done using the same procedure described above as well as a T streak assay to confirm the results of the first screen.

Gene conservation and related bioinformatic analyses

The presence of putative AHL synthases (LuxI-like) and transcriptional regulators (LuxR-like) encoding genes was determined by genome annotation and the use of different *luxI* and *luxR* homologue genes available in the databases, and which function is already experimentally validated. To study the conservation of the *colI* (coding for AHL synthase) and *colR* (coding for transcriptional regulator) DNA sequence in collimonads, a total of 9 *Collimonas* genomes (*Collimonas* sp. strain NBRC3740; *C. fungivorans* Ter331 and Ter6; *C. arenae*: Cal35, Ter10, and Ter282; *C. pratensis*: Ter91, Ter291, and PMB3(1)) were considered, in addition to seven genomes from genera taxonomically close to *Collimonas*: one belonging to the *Glaciimonas* genus (*Glaciimonas* sp. GS1), one to *Janthinobacterium*, one to *Herbaspirillum* (*H. rubrisubalbicans*), one to Massilia, one to *Burkholderia vietnamiensis*, and one to *Pseudomonas* sp. (Table 1) *Pseudomonas aeruginosa* strain PAO1 was used as outgroup. In addition, homologous genes of *colI* and *colR* were obtained by PCR from 12 *Collimonas* strains. The *colR* genes were amplified using the primers colR_sens (ATGGTTGATTGGCAAGAGCAACA) and colR_rev (CTACAAGATGCCGAGCATGGCCGC), while the *colI* genes were amplified using the primers *colI*_sens (ATGAAAGTCATTTC CGGGGCCGCCA) and *colI*_rev (TCAAGCCTCGCTCAGCGCCGATTG T). A total of 28 LuxI and LuxR protein sequences (including 20 homologues from *Collimonas* strains) were used to build a phylogenetic PhyML tree with Seaview (Gouy et al. 2010). A bootstrap analysis was based on 1000 replicates. The presence of Pfam domains was analyzed using pfam (El-Gebali et al. 2019).

Bacterial inoculum preparation

For all the functional assays described below, bacterial inocula were prepared using the same procedure. The bacterial strain PMB3(1) and its QS mutants (i.e. Δ*colI* and Δ*colR*) were grown from a −80°C glycerol stock on LB agar medium amended with gentamycin (Δ*colI* mutant) or tetracycline (Δ*colR* mutant) at 25°C for 48 h. A single colony was used to inoculate 50 ml of LB medium amended as needed with antibiotics and incubated for 48 h, while shaking (150 r/m) at 25°C. A volume of 10 ml of this culture were then collected (8000 *g*, 15 min at 4°C), washed three times in sterile water and suspended in 5 ml sterile water to obtain a suspension at OD_{595nm} (optical density at 595 nm) of 0.95 (ca. 10^9 cell/ml).

Functional assays

Different assays were performed to determine phenotypic differences between the WT PMB3(1) strain and its QS mutants. Incubations were done at 25°C for most of the assays described below, except for the confrontation with the fungus, which was done at 20°C. This temperature is determined by the growth requirements

of the fungus used and does not affect strain PMB3(1). Each assay was done with a minimum of three replicates.

Growth was determined on nutrient rich and poor media. The rich medium used was LB. The nutrient poor medium was minimal AB medium supplemented with a single carbon source (2 g/l). The carbon substrates tested were: glycerol, glucose, formate, glutamate, lysine, phenylalanine, succinate, and oxalate. The test was performed with four replicates containing 190 µl of medium and 10 µl of bacterial inoculum. Increase in optical density was followed during 120 h at 25°C at 595 nm using a TECAN microreader plate.

The utilization of sole carbon sources by the WT and QS mutant strains was analyzed with Biolog GN2 (Gram-negative) microplates used according to the manufacturer's instructions. Formazan accumulation in the bacterial cells was measured by determining the optical density at 590 nm, after 24 h incubation at 25°C, with an automatic microplate reader (Bio-Rad; model iMark).

Measurements of enzymatic activity were done according to Uroz et al. (2013). Briefly, six substrates based on 4-methylumbelliferone (MU) or 7-amino-4-methylcoumarin (AMC) were considered: MU-β-D-glucopyranoside (MU-G) for β-glucosidase (EC 3.2.1.3), MU-β-D-glucuronide hydrate (MU-GU) for β-glucuronidase (EC 3.2.1.31), MU-β-D-xylopyranoside (MU-X) for xylosidase (EC 3.2.1.37), MU-β-D-cellobioside (MU-C) for cellobiohydrolase (EC 3.2.1.91), MU-N-acetyl-β-D-glucosaminide (MU-NAG) for N-acetyl-glucosaminidase (or exochitinase; EC3.2.1.14), and L-leucine-AMC (Leu-AMC) for leucine aminopeptidase (EC 3.4.11.1) activities. All chemicals were purchased from Sigma-Aldrich Chemicals (Lyon, France). Stock solutions of each substrate (10 mM) were prepared in 2-methoxyethanol. Incubation plates contained 50 μl of incubation buffer (50 mM sodium acetate, pH = 4.5), 50 μl of bacterial suspension, and 50 μl of substrate per well. For the leucine aminopeptidase assay, the incubation buffer was Tris HCl (pH 8; 50 mM). After incubation for 1 h at 25°C, reactions were stopped by adding 50 μl of stopping buffer (Tris 1 M pH 10–11). Measurements were carried out with the Victor3 (Wallac Perkin-Elmer Life Sciences, Villebonsur-Yvette, France) with an excitation wavelength of 355 nm and an emission wavelength of 455 nm. Results were expressed in arbitrary units.

Motility was tested on solid M9 medium (20 mM NH_4Cl; 12 mM Na_2HPO_4; 22 mM KH_2PO_4; 8.6 mM NaCl; 1 mM $MgSO_4$; 1 mM $CaCl_2$,$2H_2O$; 0.2% glucose; and 0.5% casamino acids) and 0.25% agar, following the recommendation of Turnbull and Whitchurch (2014). A volume of 1 µl of bacterial inoculum was spotted on the centre of the agar in the Petri dish and colony diameters scored after 2 days.

The ability of the bacterial isolates to hydrolyze chitin was tested on minimal agar medium containing colloidal chitin (per liter: 5 g NaCl, 1 g KH_2PO_4, 0.1 g yeast extract, 20 g agar, and 2 g colloidal chitin) according to Uroz et al. (2013). A volume of 5 µl of bacterial inoculum was spotted on the center of the chitin plates. After incubation at 7 days, the clearing of the initially turbid medium indicated chitin hydrolysis and the halo diameter formed was measured.

The ability to acidify the medium was tested in minimal medium amended with glucose (2 g/l) in 96-wells microplate according to Colin et al. (2017). After 5 days of incubation, 180 µl of culture supernatant was transferred to a new microplate containing 20 µl of bromocresol green (1 g/l) per well. The pH of the culture medium was determined at 595 nm with an automatic microplate reader (Bio-Rad; model iMark) according to the method of Uroz et al. (2007).

The ability to solubilize calcium oxalate was determined in AB medium amended with 4 g calcium oxalate per liter as sole carbon source. A volume of 5 µl of bacterial inoculum was spotted onto the center of the calcium oxalate plates. After incubation for 12 days, the clearing of the initially cloudy medium indicated calcium oxalate solubilization and the halo diameters formed were measured.

The siderophore activity was performed using the liquid chrome azurol S (CAS) medium, according to Schwyn and Neilands (1987). Briefly, bacterial strains were grown in AB mannitol medium devoid of iron. After 2 days incubation, a volume of 100 µl of culture supernatant was recovered and transferred to the wells of a new microtiter plate containing 100 µl of liquid CAS medium. After 1 h of incubation at room temperature in the dark, the absorbance was measured at 655 nm with a microplate reader (Bio-Rad, model iMark).

The ectomycorrhizal fungus *Laccaria bicolor* S238N was used for the *in vitro* confrontation assay with strain PMB3(1) according to Deveau et al. (2007). The fungus was maintained on Pachlewski agar medium P5 at 20°C. A plug of *L. bicolor* S238N was cut out from the edge of a colony grown on P5 medium (0.5 g Di-NH_4 + tartrate, 1 g KH_2PO_4, 0.5 g $MgSO_4$, 20 g glucose, 5 g maltose, 1 ml 1/10 diluted Kanieltra microelement solution, 1 ml thiamine 100 mg/l solution, and 20 g agar/l at pH 5.5 for 1 l) and transferred onto the centre of a P20 plate (0.5 g Di-NH_4 + tartrate, 1 g KH_2PO_4, 0.5 g $MgSO_4$, 1 g glucose, 1 ml 1/10 diluted Kanieltra microelement solution, and 20 g agar at pH 5.5 for 1 L). A total of four 5-μl droplets of bacterial inoculum of each strain were distributed at 1.5 cm from the centre of the fungal plug of mycelium. After 15 days incubation at 20°C, colony diameter was measured and hyphal aspect and presence of bacteria on the hyphae were determined using an Olympus BX41 microscope (40x and 100x).

The effects of different treatments were assessed in R software. Data shown were means of three or four replicates. Differences between sample's means were analyzed by analysis of variance (one way ANOVA, $P < .05$, followed by a Tukey test).

RNAseq analyses

For each condition treatment (i.e. WT, Δ*colI* and Δ*colR* mutants), four flasks (i.e. replicate) were prepared. This experimental design allowed for a comparison of the transcriptomes of the WT, Δ*colI*, and Δ*colR* mutant strains. Capped Erlenmeyer flasks (100 ml) were filled with 49.5 ml of sterile LB medium, buffered at pH 6.5 by addition of 100 mM KH_2PO_4/K_2HPO_4 to avoid spontaneous hydrolysis of AHLs (Uroz et al. 2003). To each flask, 500 µl of bacterial inoculum was added, giving a total volume of 50 ml. Flasks were incubated at 25°C with agitation at 140 r/m in an orbital shaker (INFORS/Minitron). Preliminary experiments done under solid and liquid conditions showed that the WT, the Δ*colI* and Δ*colR* mutant strains grew equally well in LB medium and that 48 h corresponded to a stage of development at which the cell density was the same for all three strains and at which AHL production was clearly detected for the WT strain.

Based on this, 10 ml of culture was recovered from each flask (four replicates per treatment) after 48 h of incubation, and centrifuged at 8000 *g* (15 min; 4°C) to pellet the bacterial cells. Supernatants were removed and cells were frozen in liquid nitrogen and stored at −80°C. Total RNA was purified from each replicate (i.e. 12 samples in total) using the RiboPure™ kit (Ambion, Austin, USA) following the manufacturer's recommendations, then treated twice with DNAse I (Ambion), precipitated with ethanol, and resuspended in RNAse-free water. The concentration

Table 2. UHPLC-MS/MS quantification of AHLs produced by representative *Collimonas* strains. (A) Data are expressed in ng/ml or (B) expressed in % as the relative abundance of each AHL detected for each strain. The quantities and relative abundances of OH-forms of the AHLs are presented in bold.

A. Quantity (ng/ml)	A41	CAL40	PMB_2_3	PMB_3_1	PML_3_2	TER_10	TER_6	TER_91	TER_331
C6-HSL	0.80	2.13	1.20	5.40	4.47	0.00	3.37	5.85	4.15
C6-OH-HSL	**0.99**	**6.66**	**3.07**	**19.32**	**15.90**	**0.00**	**15.97**	**14.10**	**11.23**
C8-HSL	0.22	1.79	0.65	1.96	1.35	0.00	2.93	1.64	2.82
C8-OH-HSL	**0.00**	**14.04**	**0.00**	**16.20**	**13.19**	**0.00**	**25.22**	**14.73**	**20.83**
C10-OH-HSL	**0.19**	**6.66**	**0.62**	**1.73**	**1.39**	**0.59**	**11.45**	**1.70**	**9.77**
C10-oxo-HSL	0.00	0.10	0.00	0.00	0.00	0.03	0.19	0.00	0.39
C12-OH-HSL	**0.00**	**0.52**	**0.10**	**0.49**	**0.00**	**1.43**	**0.84**	**0.47**	**0.00**
C12-oxo-HSL	0.00	0.00	0.00	0.00	0.00	0.72	0.08	0.00	0.10
B. Relative abundance (%)	**A41**	**CAL40**	**PMB_2_3**	**PMB_3_1**	**PML_3_2**	**TER_10**	**TER_6**	**TER_91**	**TER_331**
C6-HSL	36.2	6.7	21.2	12.0	12.3	0.0	5.6	15.2	8.4
C6-OH-HSL	**45.0**	**20.9**	**54.5**	**42.9**	**43.8**	**0.0**	**26.6**	**36.6**	**22.8**
C8-HSL	10.1	5.6	11.6	4.3	3.7	0.0	4.9	4.2	5.7
C8-OH-HSL	**0.0**	**44.0**	**0.0**	**35.9**	**36.3**	**0.0**	**42.0**	**38.3**	**42.3**
C10-OH-HSL	**8.7**	**20.9**	**11.0**	**3.8**	**3.8**	**21.4**	**19.1**	**4.4**	**19.8**
C10-oxo-HSL	0.0	0.3	0.0	0.0	0.0	1.2	0.3	0.0	0.8
C12-OH-HSL	**0.0**	**1.6**	**1.7**	**1.1**	**0.0**	**51.5**	**1.4**	**1.2**	**0.0**
C12-oxo-HSL	0.0	0.0	0.0	0.0	0.0	25.9	0.1	0.0	0.2

and quality of the extracted RNA were assessed using a Nanodrop 2000 spectrophotometer (Thermo Scientific, Waltham, MA, USA), a Qubit® RNA Assay Kit in a Qubit® 2.0 Fluorometer (Life Technologies, CA, USA), and TapeStation analyses. The RNA integrity number value was 9.0 on average. RNA preparations were sent to GENEWIZ which operated the rRNA depletion using the Ribo-Zero rRNA removal kit for bacteria, performed the stranded RNA library preparation and sequenced the cDNA on their Illumina HiSeq2500 platform using a 2 × 150bp paired-end (PE) configuration in High Output mode (V4chemistry). This sequencing generated a total of more than 295 million reads ranging from 25 to 31 million per sample.

RNAseq reads were mapped to the coding sequences (CDS) of the genome of strain PMB3(1) through the MICROSCOPE (Vallenet et al. 2019) annotation platform using the BWA (version 0.7.4-r385; Li and Durbin 2009). The DESeq2 package (Anders and Huber 2010, Love et al. 2014) was used to calculate differential gene expression abundance between the different treatments. A normalization of read numbers for replicates in each treatment was performed (by estimates of size factors in DESeq2 and normalization), then differential expression values (FoldChange) and statistical values (pVal and adjusted pVal through the Benjamini and Hochberg's approaches) assessing the false discovery rate (FDR) were calculated. All genes having an adjusted *P*-value less than to .05, a base mean score ≥ 150 a cut-off for absolute fold change ≥ 0.9 were considered as significantly differentially expressed. The genes differentially expressed were sorted according to the genome sequence of strain PMB3(1) (WXXL00000000) and raw data statistics are accessible on the SRA platform (PRJNA787782). In addition, treatment comparison was performed using the Mixomics R package (González et al. 2012, Rohart et al. 2017). To do this, the full raw dataset was first normalized to identify the genes that were present above a threshold of 100 in the RNAseq dataset in one of the treatments considered. A Partial Least Squares (PLS) regression was first done to integrate the RNAseq matrix of the WT vs. ΔQS mutants to generate a global view. PLS is a robust multivariate projection-based method used to explore or explain the relationship between two continuous datasets. To allow interpretability a Sparse Partial Least Squares regression (sPLS) was then performed as it permits to perform simultaneous variable selection. The distribution of the different genes considered was then visualized in a correlation circle plot permitting to evidence treatment specific genes. The list of genes was then compared to the outputs of the DESeq2 analysis.

Results

Identification of AHLs produced by *C. pratensis* PMB3(1) and other collimonads

Except for strains Ter10 and Ter282, all of the tested *Collimonas* strains (Table 1; Figure S2, Supporting Information) triggered violacein production in a streak assay with the biosensor *C. violaceum* CV026. Concentrated extracts recovered from cultures of Ter282 and Ter10 produced a positive signal with strain Ter282, but not with Ter10. TLC analyses revealed similar patterns for all strains that scored positive in the streak assay, but with variation in the intensity of the spots detected. A comparison with standards identified these two compounds as 3OHC6-HSL (detected with both types of biosensor) and 3OHC8-HSL (only detected by *Agrobacterium*; data not shown). The UHPLC-MS/MS analyses done on strain PMB3(1) and a subset of *Collimonas* strains [i.e. A41, Cal40, and PMB2(3), PML3(2), Ter10, Ter6, Ter91, and Ter331] provided qualitative and quantitative information on the AHLs produced. This approach revealed the presence of AHLs in each strain, but in very low quantities in strains Ter10 and A41 (i.e. below 1 ng/ml; Table 2). Consistent with the TLC results, 3OHC6-HSL and/or 3OHC8-HSL were the two main molecules, followed by 3OHC10-HSL (Figure S1, Supporting Information). These three AHLs represented in relative abundance of AHLs detected between 45% and 80% of the total. Concentrations of 19.3 ng/ml for 3OHC6-HSL and 16.2 ng/ml 3OHC8-HSL were determined for strain PMB3(1). Unsaturated forms of (C6, C8, and C10-HSL) were also detected, but at lower concentrations than their related OH form. The single exception was strain Ter10 for which only low quantities of 3OHC10-HSL (0.5 ng/ml) and 3OHC12-HSL

(1.4 ng/ml) were detected as well as their corresponding oxo forms.

Identification of the region involved in AHL production in *C. pratensis* PMB3(1)

As strain PMB3(1) was positive for the production of AHLs, its genome was used to identify the putative AHL synthases and QS-related LuxR regulators using several characterized LuxI/LuxR from the databases. This analysis allowed us to identify a single *luxI–luxR* gene pair, with the gene *colI* encoding a putative AHL synthase gene and the gene *colR* encoding a putative QS-related LuxR regulator in its close vicinity (Figure S2, Supporting Information). We also identified six proteins with a LuxR-like domain (HTH), but with low identity with known LuxR proteins. The open reading frames of both *colI* and *colR* showed upstream sequences with reasonable matches to a consensus ribosome binding site (RBS) sequences and −10 and −35 promoter elements. Within the intergenic region of 212 bp that separated the *colI* and *colR* open reading frames, we found a palindromic sequence of 28 nt (Figure S2A, Supporting Information) representing the typical characteristics of a lux box and a putative binding site for the ColR protein.

Sequence analysis of the *colI* gene predicted a protein of 225 amino acids in length. Blast analyses revealed high homology of this protein with putative AHL synthases or acyl-CoA *N*-acyl transferases belonging to collimonads and related genera. Amino acid sequence identity ranged from 72% to 100% with other *Collimonas* strains, but was only 66% or even lower with *Glaciimonas immobilis* (WP_168057061.1), *Massilia* sp. (WP_112936725.1), and *Janthinobacterium lividum* (WP_139090813.1). Sequence analysis of the *colR* gene predicted a protein product with a length of 237 aa. A pfam analysis revealed the presence of two domains, an autoinducer domain and a LuxR domain. Amino acid sequence identity of the *colR* gene product with other collimonads ranged from 78% with Ter10 to 100% with the other strains, but decreased to 64% or lower with *Glaciimonas* (WP_153234475.1) or *Massilia* (WP_169468232.1) or *Janthinobacterium* (WP_099414465.1). All other luxR-like homologues found in strain PMB3(1) lack a significant autoinducer domain, suggesting that they are not bona fide coding for a LuxR regulator.

The predicted function of the *colI* gene of strain PMB3(1) was confirmed by showing that a Δ*colI* knockout mutant did not produce any AHLs in both streak assay (Figure S2B, Supporting Information) and TLC analysis done on concentrated extracts. For a Δ*colR* knockout mutant, AHL production was just above the limit of detection in the first 24 h, whereas no AHL accumulation was observed after 2 days or longer incubation period. For both mutants, the ability to produce AHLs was restored after complementation with plasmids carrying the *colI* or *colR* gene, respectively (data not shown).

Conservation of colI and colR among collimonads

Homologous LuxI AHL synthase and LuxR-like transcriptional regulator protein sequences were identified through the analysis of a set of *Collimonas* genomes available in the databases or through a PCR/sequencing approach. All the *Collimonas* tested in our study harboured a single pair of *colI* and *colR* homologues in their genome as the strain PMB3(1). The relatedness of the ColI and ColR proteins between collimonads was confirmed by the construction of phylogenetic trees (Fig. 1A and B). From these trees, we conclude that the ColI and ColR trees phylogenies were congruent with the phylogenetic affiliation (i.e. *C. arenae*, *C. fungivorans*, and *C. pratensis*). A single exception was observed for strain Ter10 that harboured an atypical ColR–like protein sequence of only 47 aa. Noticeably, all the genes encoding putative AHL synthases cloned in pGEM-T conferred to *E. coli* the ability to activate the biosensor CV026, including the AHL synthase from strain Ter10 (data not shown).

Functional assays done on *C. pratensis* PMB3(1)

A set of functional assays done on the WT strain and its Δ*colI* and Δ*colR* mutants provides information on how QS affects the physiology and metabolism of strain PMB3(1) (Fig. 2)

Growth curves were compared to determine whether the WT and the mutant strains differed. On nutrient rich media, the two mutants tended to grow better than the WT strain (Fig. 2A). In contrast, under nutrient-poor conditions, significant differences were observed between WT and mutants in terms of yield. Noticeably, while the mutants reached higher cell densities than WT in presence of glucose (Fig. 2B), a significantly higher acidification activity was observed for the WT strain (pH_{WT}: 4 ± 0.04 vs. $pH_{\Delta luxI}$: 4.7 ± 0.04 and $pH_{\Delta luxR}$: 4.4 ± 0.12; $P < .05$; Fig. 2C). In presence of formate as the sole carbon source, the WT strain was not able to grow, while the mutants presented a weak but significantly higher growth (Fig. 2D). No differences were observed for the other carbon sources tested as sole carbon source (i.e. glycerol, glutamate, lysine, phenylalanine, and succinate) and no growth was observed for either WT or mutants with oxalate in liquid condition. The GN2 BIOLOG assay revealed significant differences between the WT and mutant strains, with γ-Hydroxybutyric acid, -Glutamic acid, -Serine, Xylitol, and -Galactose significantly more metabolized by the WT strain (Figure S3, Supporting Information).

Other functional assays revealed that the QS mutants were strongly impaired in their motility compared to the WT strain (Fig. 2E) and presented a significantly higher leucine aminopeptidase activity than the WT strain ($P < .05$; Fig. 2F). No significant differences were observed for the solubilization of calcium oxalate and inorganic phosphorus on solid media, although the mutants looked slightly more effective in both assays. Noticeably, while no growth was observed on the oxalate growth assay in liquid culture (presented above), a halo was formed on solid medium. No difference was observed between the different strains concerning the ability to mobilize iron, to hydrolyze chitin as well as in the ability to inhibit the growth of *L. bicolor* (Table S2 and Figure S4, Supporting Information).

Transcriptome statistics and overview of the variations in the COGs

After 48 h incubation in liquid LB medium (buffered at pH 6.5), transcriptome profiling was conducted by RNA-Seq to identify the differentially expressed genes (DEGs) in strain PMB3(1) in a QS-dependent way by comparison of the WT strain to the Δ*colI* and Δ*colR* mutants. After barcode removal and quality control, the number of reads retained varied from 23 to 31 million per replicate, giving a total of 96 Gb of 150 bp PE sequence data. Between 61.32% and 90% of reads mapped at least once on the genome of *C. pratensis* PMB3(1). After the removal of the unmapped sequences and of the remaining rRNA sequences, between 50% and 87% of the total number of reads were retained per sample. A total of 1112 and 814 DEG with a significant adjusted *P*-value were detected in Δ*colI*/WT and Δ*colR*/WT treatment comparisons (corresponding to 20.3% and 14.8% of the genes of strain PMB3(1)), respectively. When a cut-off for absolute fold change > 0.9 (log2FC) was applied, the number of DEGs was 220 and 153 in the Δ*colI*/WT

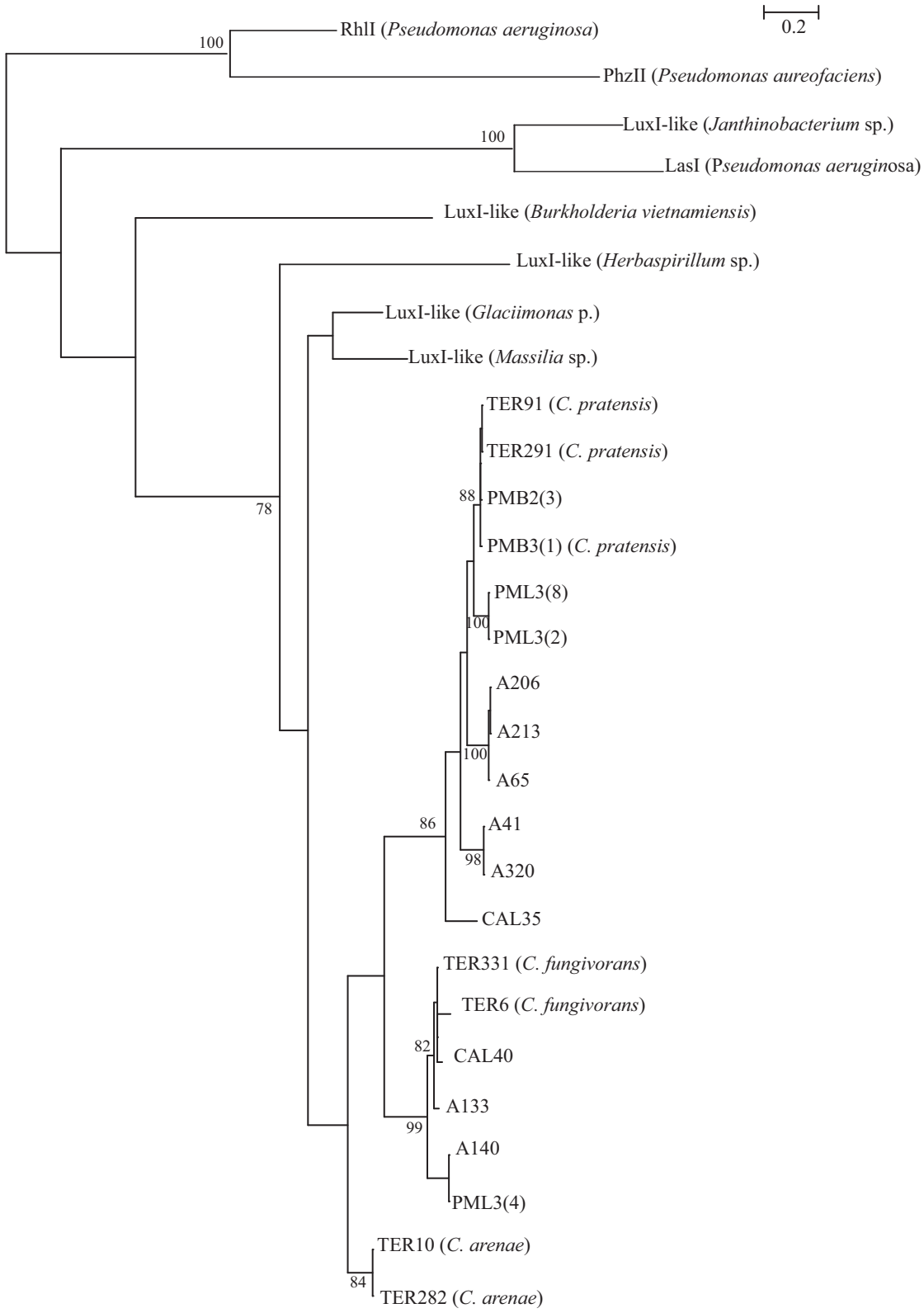

Figure 1. Phylogenetic tree analyses. **(A)** Autoinducer synthase from strain PMB3(1) and other *Collimonas* species. **(B)** Transcriptional regulator from strain PMB3(1) and other *Collimonas* species. The numbers at the node show the bootstrap values as a percentage of 1000 bootstrap replications.

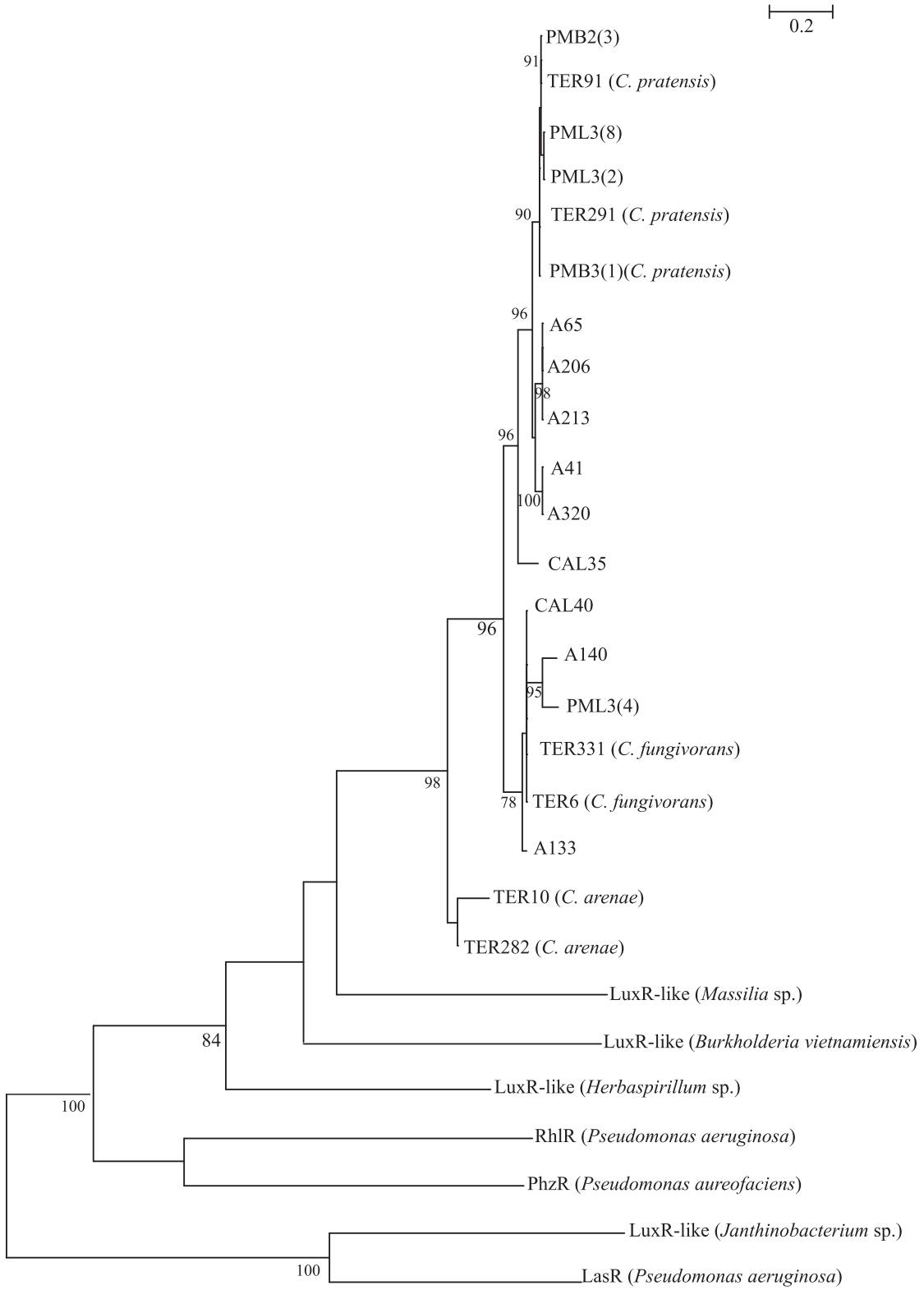

Figure 1. *Continued.*

and Δ*colR*/WT treatment comparisons (corresponding to 4% and 2.8% of the genes of strain PMB3(1)), respectively. Noticeably, all the genes found as significantly regulated in one treatment comparison were also found in the other, but with a log2change value sometime lower than 0.9 (absolute value). Genes that were differentially regulated (log2FC ≥ 0.9 absolute value) and found in both RNAseq datasets (Δ*colI*/WT and Δ*colR*/WT) are presented in Table 3. Applying these criteria to the Δ*colI*/Δ*colR* treatment comparison revealed that the two expression profiles of the Δ*colI* and Δ*colR* mutants were very similar. Only four DEGs with low

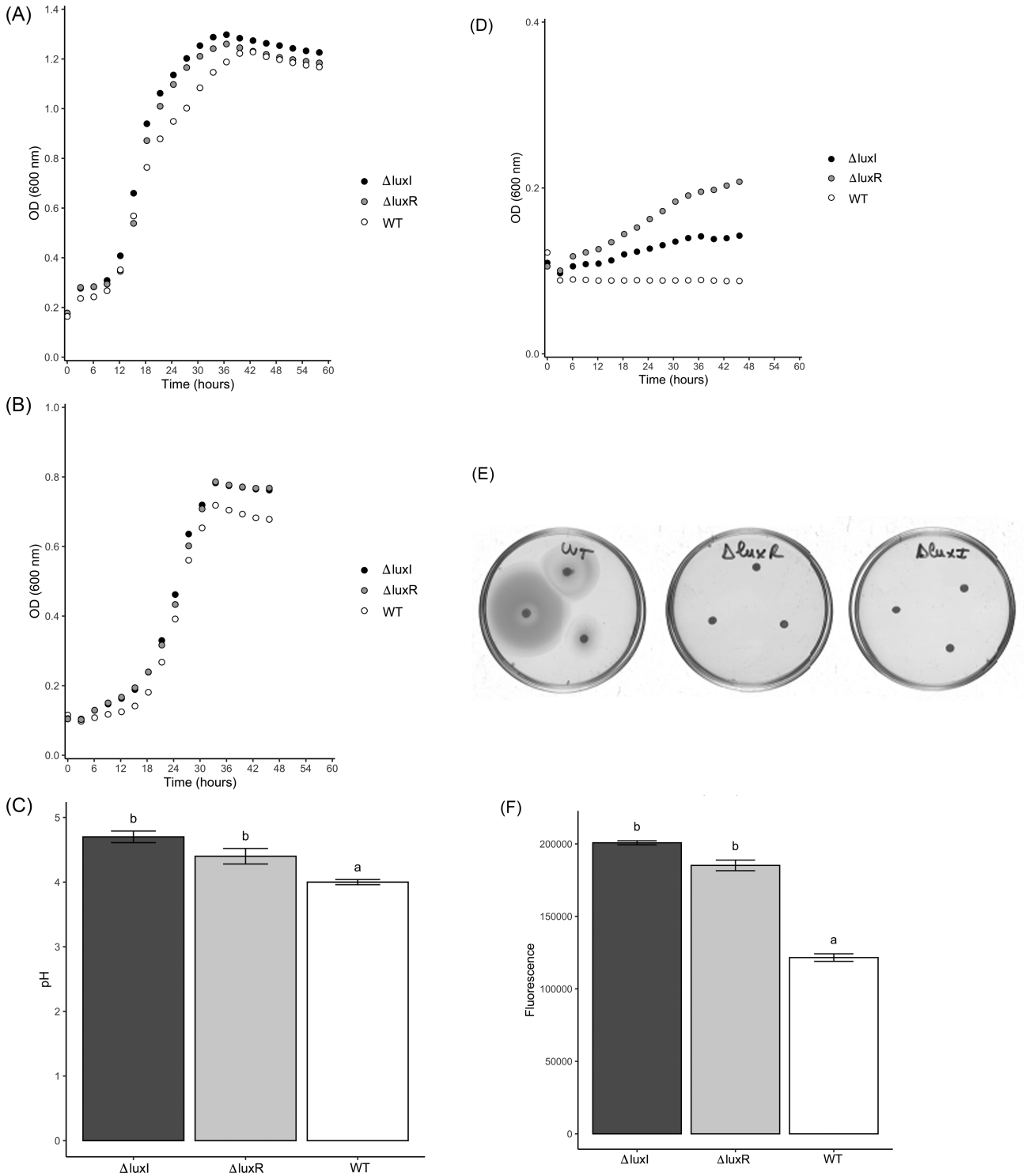

Figure 2. Functional assays. **(A)** Growth in rich medium (OD600nm); **(B)** growth in nutrient-poor medium with glucose as sole C source (OD600nm); **(C)** acidification assay (presenting solution pH); **(D)** growth in nutrient-poor medium with formate as sole C source (OD600nm); **(E)** motility assay, and **(F)** leucin aminopeptidase assay. For each bioassay, the colour code is presented as follows: white, WT; black, Δ*luxI*, and Grey, Δ*luxR*. Treatments with different letters indicate significant difference according a one-factor ANOVA ($P < .05$).

sequence coverage and poorly or uncharacterized functions differed.

The comparison of the different treatments through a sPLS (MIxOMICs) confirmed the DESeq2 analysis showing that the Δ*colI* and Δ*colR* mutants clustered together. The MIxOMICs analysis also strongly highlighted how the QS mutants differed from the WT strain (Fig. 3). The strong relationship between the DEGs obtained in each treatment comparison (i.e. Δ*colI*/WT vs. Δ*colR*/ WT) was also evidenced through a linear regression analysis ($y = 1.1x-0.24$; $P < .0001$; $R^2 = 0.85$; Fig. 4). Such correlation evidenced that the down- and up-regulated genes followed the same trend in the two treatment comparisons (i.e. (Δ*colI*/WT and Δ*colR*/WT).

Table 3. Genes shared between the RNAseq treatment comparisons (i.e. ΔluxI/WT vs. ΔluxR/WT). For legibility, only the genes presenting a log2fold change ≥ 0.9 (absolute value) in one of both analysis methods are presented. The normalized number of reads per comparison is presented. The NCBI gene Id is presented for each gene. The grey zone in the table allows to differentiate up- and down-regulated genes.

		Comparison WT vs. ΔluxI			Comparison WT vs. ΔluxR		
Gene_ID	Product	Log2FC	ΔLuxI	WT	log2FC	ΔluxR	WT
NKI71559.1	Phenylalanine-4-hydroxylase	−3.11	25 655	2963	−2.88	24 412	3321
NKI69684.1	Conserved protein of unknown function	−2.96	6631	855	−2.74	6407	959
NKI71429.1	Ornithine aminotransferase	−2.89	5179	697	−2.90	5816	781
NKI72184.1	Flp/Fap pilin-like protein	−2.74	1344	202	−3.03	1845	226
NKI68220.1	Saccharopine Dehydrogenase/Lysine 6-dehydrogenase	−2.46	9616	1749	−2.37	10 134	1961
NKI69683.1	Putative alpha-1,3-mannosyltransferase MNN12	−2.41	1520	287	−2.46	1771	322
NKI71428.1	Putative N-Dimethyline dimethylaminohydrolase	−2.38	2982	572	−2.38	3346	642
NKI72183.1	Transcriptional regulator, MerR family	−2.28	305	63	−2.58	421	71
NKI71944.1	Conserved protein of unknown function	−2.26	1958	408	−2.24	2158	458
NKI71945.1	Putative oxidoreductase protein	−2.13	3018	688	−2.02	3125	771
NKI72395.1	Transporter	−2.10	1578	367	−3.04	3373	411
NKI70105.1	Porin, Gram-negative type	−1.97	21 367	5466	−2.44	33 217	6127
NKI68292.1	Conserved protein of unknown function	−1.90	594	160	−1.64	560	179
NKI67908.1	Formate dehydrogenase-O, cytochrome b556 subunit	−1.87	207	56	−2.77	429	63
NKI70782.1	Fused DNA-binding transcriptional regulator	−1.87	664	182	−2.57	1211	204
NKI71006.1	Conserved hypothetical protein	−1.85	2033	562	−1.90	2360	630
NKI67909.1	Formate dehydrogenase-O, Fe-S subunit	−1.84	561	156	−2.71	1148	175
NKI70108.1	Glucose-6-phosphate dehydrogenase	−1.75	1742	518	−2.37	2998	581
NKI70143.1	-proline glycine betaine binding ABC transporter protein proX	−1.67	1022	322	−1.91	1351	361
NKI72388.1	Putative Chitooligosaccharide deacetylase uricase	−1.67	1450	457	−2.35	2608	513
NKI71007.1	Conserved protein of unknown function	−1.64	1679	539	−1.88	2227	604
NKI68260.1	Diaminopimelate decarboxylase, PLP-binding	−1.63	479	155	−1.11	374	174
NKI69958.1	5-Methyltetrahydropteroyltriglutamate-homocysteine S-methyltransferase	−1.62	27 344	8904	−1.68	31 950	9981
NKI70144.1	Choline-sulfatase	−1.57	1378	465	−1.82	1844	521
NKI71254.1	Protein of unknown function	−1.55	264	91	−1.94	391	102
NKI70107.1	Putative Bifunctional protein glk [Includes: Glucokinase	−1.49	1380	491	−2.03	2242	550
NKI70162.1	Putative sugar transport protein	−1.47	1074	389	−1.29	1063	436
NKI69951.1	Putative Permease, multidrug-efflux transporter	−1.45	520	191	−1.76	723	214
NKI70796.1	Glucose/Gluconate/Sorbitol 2-dehydrogenase cytochrome subunit	−1.44	414	152	−2.20	782	171
NKI71935.1	Putative Pilus biogenesis protein tapA /pilA or pilD	−1.44	26 116	9609	−1.42	28 728	10 768
NKI71947.1	Histidine ammonia-lyase (fragment)	−1.42	216	81	−2.26	433	90
NKI72821.1	Aldehyde dehydrogenase B	−1.42	18 336	6877	−1.23	18 029	7710
NKI67910.1	Formate dehydrogenase-O major subunit (fragment)	−1.37	1865	720	−2.10	3473	808
NKI72389.1	Porin	−1.36	4033	1577	−1.78	6052	1767
NKI71688.1	Type IV pilus biogenesis protein PilM	−1.35	486	192	−1.34	544	215
NKI68126.1	Conserved membrane protein of unknown function	−1.34	260	102	−1.64	359	115
NKI72206.1	Protein of unknown function	−1.33	416	165	−2.59	1117	185
NKI69905.1	5-hydroxyisourate hydrolase	−1.32	1334	535	−2.08	2541	600
NKI70229.1	Fimbrial chaperone protein	−1.32	486	195	−1.85	791	219
NKI72387.1	Conserved protein of unknown function	−1.32	2672	1073	−2.20	5514	1203
NKI72393.1	Conserved membrane protein of unknown function	−1.30	1301	529	−2.20	2725	593

Table 3. Continued

Gene_ID	Product	Comparison WT vs. ΔluxI			Comparison WT vs. ΔluxR		
		Log2FC	ΔLuxI	WT	log2FC	ΔluxR	WT
NKI69367.1	Catalase	−1.28	299	123	−1.42	370	138
NKI68462.1	Phosphopantetheine-binding	−1.27	269	111	−2.30	614	125
NKI69613.1	Conserved protein of unknown function	−1.25	8626	3619	−1.50	11 462	4057
NKI69906.1	Fimbrial subunit	−1.25	3419	1440	−1.88	5955	1615
NKI68169.1	Conserved protein of unknown function	−1.23	419	179	−1.34	509	201
NKI72540.1	Conserved protein of unknown function	−1.22	457	197	−2.43	1187	220
NKI68263.1	Protein of unknown function	−1.19	4596	2015	−1.61	6876	2259
NKI70980.1	8-oxoguanine deaminase	−1.18	1448	639	−1.86	2600	716
NKI72397.1	DNA-binding domain-containing protein, AraC-type	−1.18	1615	712	−1.55	2334	798
NKI72396.1	N-carbamoyl-L-amino-acid hydrolase	−1.17	1967	872	−1.94	3745	978
NKI69446.1	Oxalyl-CoA oxalate decarboxylase	−1.15	843	380	−2.40	2246	426
NKI70073.1	Conserved protein of unknown function	−1.14	736	335	−2.44	2039	376
NKI71871.1	Conserved protein of unknown function	−1.13	284	129	−2.04	598	145
NKI71331.1	Type IV pilus biogenesis protein PilO	−1.12	325	151	−1.13	368	169
NKI71690.1	D-amino acid dehydrogenase, small subunit can act on leucine	−1.12	1803	832	−1.31	2309	932
NKI68168.1	Oxidative demethylase	−1.10	411	192	−1.21	498	215
NKI69705.1	Conserved exported protein of unknown function	−1.09	546	256	−1.48	799	287
NKI70797.1	Glutaminase/Asparaginase	−1.09	2485	1168	−1.49	3687	1310
NKI71691.1	Type IV pilus biogenesis protein PilP	−1.08	301	142	−1.20	368	160
NKI68680.1	Periplasmic binding protein TonB	−1.07	1464	701	−1.36	2018	786
NKI69257.1	Putative sugar transporter subunit (ABC transporter)	−1.05	481	233	−1.11	562	261
NKI71509.1	6,7-dimethyl-8-ribityllumazine synthase 2	−1.04	393	192	−1.10	461	215
NKI72575.1	Putative transporter	−1.04	219	106	−1.74	398	119
NKI68064.1	Putative acetyltransferase	−1.00	477	239	−1.53	775	268
NKI68064.1	Protein of unknown function	−1.00	204	103	−1.65	362	115
NKI68264.1	Protein of unknown function	−1.00	204	103	−1.65	362	115
NKI68166.1	Fused DNA-binding transcriptional dual regulator	−0.99	568	286	−1.25	762	320
NKI69483.1	Conserved exported protein of unknown function	−0.98	2231	1129	−1.14	2786	1267
NKI70908.1	Transcriptional regulator	−0.98	1909	970	−1.47	3019	1087
NKI70540.1	Oxidoreductase (Flavoprotein)	−0.96	1541	794	−1.53	2577	891
NKI70781.1	Alkyl hydroperoxide reductase, C22 subunit (detoxification of hydroperoxides)	−0.94	12 584	6555	−1.09	15 629	7349
NKI71597.1	Succinate-semialdehyde dehydrogenase I, NADP-dependent	−0.93	1497	786	−1.47	2438	881
NKI71934.1	Putative Fimbrial assembly protein, serogroup E1	−0.93	366	194	−1.41	572	217
NKI71936.1	Conserved protein of unknown function	−0.91	914	487	−1.02	1108	546
NKI68315.1	Succinyl-CoA synthetase, beta subunit	0.90	8255	15 411	1.19	7566	17 282
NKI71939.1	Threonine efflux protein	0.90	1785	3338	0.96	1929	3743
NKI68341.1	Ferrichrome-iron receptor	0.92	4531	8544	1.26	3991	9578
NKI69091.1	Multidrug efflux system protein	0.93	519	988	0.94	579	1108
NKI68080.1	Protein PecM	0.96	331	642	1.20	314	720
NKI68080.1	Major capsid protein	0.96	272	531	0.97	304	595
NKI68725.1	Major capsid protein	0.96	272	531	0.97	304	595
NKI70599.1	Periplasmic serine endoprotease DegP-like	0.97	1146	2234	1.14	1139	2505
NKI69918.1	Molybdenum ABC-transporter	0.98	456	897	1.08	475	1005
NKI69023.1	Acetohydroxy acid isomeroreductase/2-dehydropantoate 2-reductase	1.02	10 083	20 439	1.12	10 572	22 916
NKI70380.1	Molecular chaperone HSP90 family	1.02	9364	19 039	1.08	10 132	21 346
NKI69695.1	2-oxoglutarate decarboxylase, thiamin-requiring	1.03	23 273	47 344	1.12	24 412	53 083
NKI70541.1	Lead, cadmium, zinc, and mercury transporting ATPase	1.04	1257	2579	1.03	1416	2892

Table 3. Continued

Gene_ID	Product	Comparison WT vs. ΔluxI			Comparison WT vs. ΔluxR		
		Log2FC	ΔLuxI	WT	log2FC	ΔluxR	WT
NKI71957.1	Conserved protein of unknown function	1.05	20 270	42 052	1.28	19 387	47 156
NKI69924.1	ABC transporter, ATP-binding protein	1.07	2935	6156	1.11	3193	6903
NKI69973.1	conserved protein of unknown function	1.08	5595	11 796	1.29	5395	13 221
NKI70816.1	Cold-shock DNA-binding domain protein	1.10	889	1908	1.01	1061	2140
NKI69694.1	dihydrolipoyltranssuccinase	1.12	16 620	36 153	1.15	18 216	40 537
NKI69460.1	Sugar transferase	1.14	161	355	0.95	205	398
NKI69923.1	NADP-specific glutamate dehydrogenase	1.16	3972	8892	1.16	4472	9970
NKI71381.1	Conserved protein of unknown function	1.17	7475	16 841	1.14	8576	18 883
NKI71885.1	Putative lactam utilization protein, UPF0271 family	1.17	976	2201	1.17	1095	2468
NKI72719.1	chaperone Hsp60, peptide-dependent ATPase, heat shock protein	1.19	34 707	78 996	1.34	34 942	88 574
NKI69060.1	Negative regulator of PhoR/PhoB two-component regulator	1.26	240	575	1.31	260	645
NKI68500.1	Conserved exported protein of unknown function	1.29	1217	2980	1.24	1411	3342
NKI69940.1	Putative Isocitrate lyase/ malate synthase	1.33	9194	23 120	1.39	9922	25 927
NKI71377.1	Pyrrolidone-carboxylate peptidase	1.36	386	989	1.21	478	1109
NKI69057.1	Phosphate transporter subunit	1.37	199	514	1.47	207	576
NKI71380.1	Conserved protein of unknown function	1.39	455	1191	1.35	525	1336
NKI69056.1	Protein YdeP	1.45	964	2626	1.69	910	2944
NKI71849.1	Phosphate transporter subunit	1.45	718	1964	1.80	634	2202
NKI71848.1	Conserved protein of unknown function	1.49	233	654	1.78	213	733
NKI69058.1	Conserved protein of unknown function	1.53	422	1216	1.37	527	1364
NKI71378.1	Phosphate transporter subunit	1.53	207	597	1.83	188	670
NKI68213.1	ThiJ/PfpI family protein	1.56	272	800	1.88	243	897
NKI69810.1	Membrane-associated Zn-dependent endopeptidase	1.56	10 643	31 439	1.48	12 648	35 254
NKI69922.1	4-hydroxyphenylpyruvate dioxygenase	1.59	3130	9444	1.58	3545	10 590
NKI69059.1	Phosphate transporter subunit	1.60	247	748	1.66	266	839
NKI71379.1	Putative membrane protein	1.60	682	2063	1.38	889	2313
NKI68856.1	Magnesium transporter	1.93	197	746	1.98	212	837
NKI68380.1	Conserved protein of unknown function	2.01	5326	21 421	1.67	7559	24 016
NKI72377.1	Extracellular protease	2.32	480	2398	2.09	632	2688
NKI68381.1	Modulator of FtsH protease YccA	2.37	4254	21 930	2.06	5906	24 589
NKI69241.1	Lytic polysaccharide monooxygenase/ GlcNAc-binding protein A (fragment)	3.44	83	902	3.25	106	1011

The assignment of DEGs of *C. pratensis* PMB3(1) into the clusters of orthologous groups (COG) categories revealed that the DEGs were mostly assigned to amino acid transport and metabolism (category E; Δ*colI*/WT: 16.5% vs. Δ*colR*/WT: 14%), inorganic ion transport and metabolism (category P; Δ*colI*/WT: 11.4% vs. Δ*colR*/WT: 7.5%), and Energy production and conversion (category C; 8.9% for each comparison). For most of these categories, the QS-mutants (Δ*colI* and Δ*colR*) presented higher percentages of up regulated COG genes than the WT, except for post-translational modification, protein turnover, chaperones (category O; 0.6%–0.9% up vs. 3.7%–3.8% down).

Transcriptional changes linked to the mutation of colI and colR as compared to the WT strain

A focus on the expression of *colI* or *colR* in the QS-mutants revealed that in the Δ*colR* mutant the expression of *colI* was suppressed compared to the WT strain (NKI69496.1; log2FC:–2.6), suggesting that *colI* expression is under the positive control of *colR*. In the Δ*colI* mutant, the expression of *colR* appeared increased in comparison to the WT strain (NKI69495.1; log2FC:0.95).

Because the ΔcolI/WT and ΔcolR/WT treatment comparisons showed the same trends for DEGs (i.e. linear regression analysis presented above), the Δ*colI* and Δ*colR* data were pooled and termed QS-mutants. A comparison between the WT strain and the QS-mutants is presented below. For legibility reasons, up- and down-regulated gene expressions in the QS-mutants are presented separately. Some of these genes code for the synthesis of putative metabolites by strain PMB3(1), as predicted by AntiSMASH.

Down-regulated gene expression in QS-mutants

Several genes related to phosphate access, amino acid degradation and other proteolytic activities appeared down-regulated in the QS-mutants. Genes encoding homologues of the phosphate (*pho*) regulon showed lower expression levels in the QS-mutants than in the WT strain. The genes *pstA*, *B*, *C*, and *S* (NKI69056.1-NKI69059.1), which are involved in phosphate specific transport (*pst*) presented a log2C of −1.37 to −1.60. The gene *phoU* (NKI69060.1) presented a log2C: −1.26. PhoU is a regulatory protein that interacts with PstB and PhoB to regulate the import of inorganic phosphorus (Pi) through the Pst system. It plays a crucial role in the regulation of P homeostasis.

Several other enzymes or transporters were downregulated in the QS mutants, e.g. the gene NKI69241.1 (log2C: −3.44),

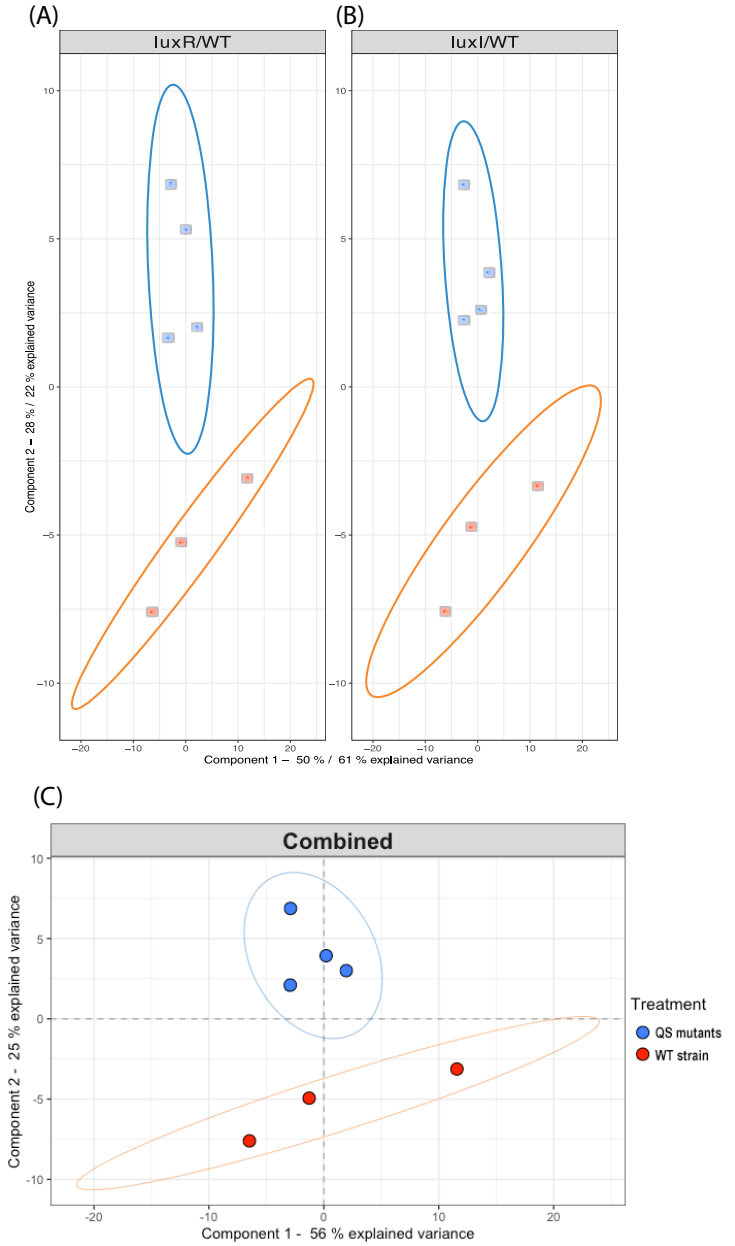

Figure 3. Multivariate analyses the transcriptomic data. Visualization of sPLS sample projection plots according to (A) Δ*luxR*/WT RNAseq data, (B) Δ*luxI*/WT RNAseq data, and (C) combined (RNAseq of the two mutants /WT) data (C). In each panel (A), (B), and (C), the colour code is: WT, red; mutant, blue. Confidence ellipses for each treatment are plotted to highlight the strength of the discrimination (confidence level set to: 95%).

which encodes a lytic polysaccharide monooxygenase that possesses a GlcNAc-binding domain allowing binding to proteins and chitin; genes coding for an extracellular protease [NKI72377.1 (EC 3.4.24.) log2C: −2.32] or an endopeptidase (NKI69810.1, log2C: −1.56); genes coding for enzymes involved in the 2-oxoglutarate degradation pathway [NKI69694.1, *sucB* homologue (EC 2.3.1.61) and NKI69695.1, *sucA* homologue (EC 1.2.4.2)] and phenylalanine degradation pathway [NKI69922.1 (EC 1.13.11.27), NKI69923.1 (EC 1.4.1.3), and NKI69924.1 (EC 3.6.3.25); log2c: −1 to −1.5]; as well as a potential iron transporter related to the ferrichrome (NKI68341.1; log2C: −0.92).

Noticeably, several QS down-regulated genes in strain PMB3(1) were identified in an independent AntiSMASH analysis. A single gene (NKI69940.1; log2c: −1.33) encoding an isocitrate lyase was identified as member of the NRPS cluster #6, a cluster predicted to produce a peptide (ile—ser—ile). A total of five genes belonging to the thiopeptide cluster #11 were down-regulated and corresponded to genes encoding a pyrrolidone carboxyl peptidase (EC 3.4.11.8; NKI71377.1, log2C: −1.36), a lactam utilizing protein (NKI71381.1), encoding a hydrolase (NKI71382.1) or unknown proteins (NKI71378.1–NKI71380.1)

Up-regulated gene expression in QS-mutants

Several genes involved in oxalate and formate metabolism appeared up-regulated in the QS-mutants. Some of these genes were organized into two separate regions on the PMB3(1) genome. The first region encompasses four genes described in other taxa as responsible for oxalate metabolism with the genes NKI69443.1 and NKI69445.1 encoding two formyl-CoA transferases (EC 2.8.3.16), NKI69446.1 encoding an oxalyl-CoA oxalate decarboxylase (EC

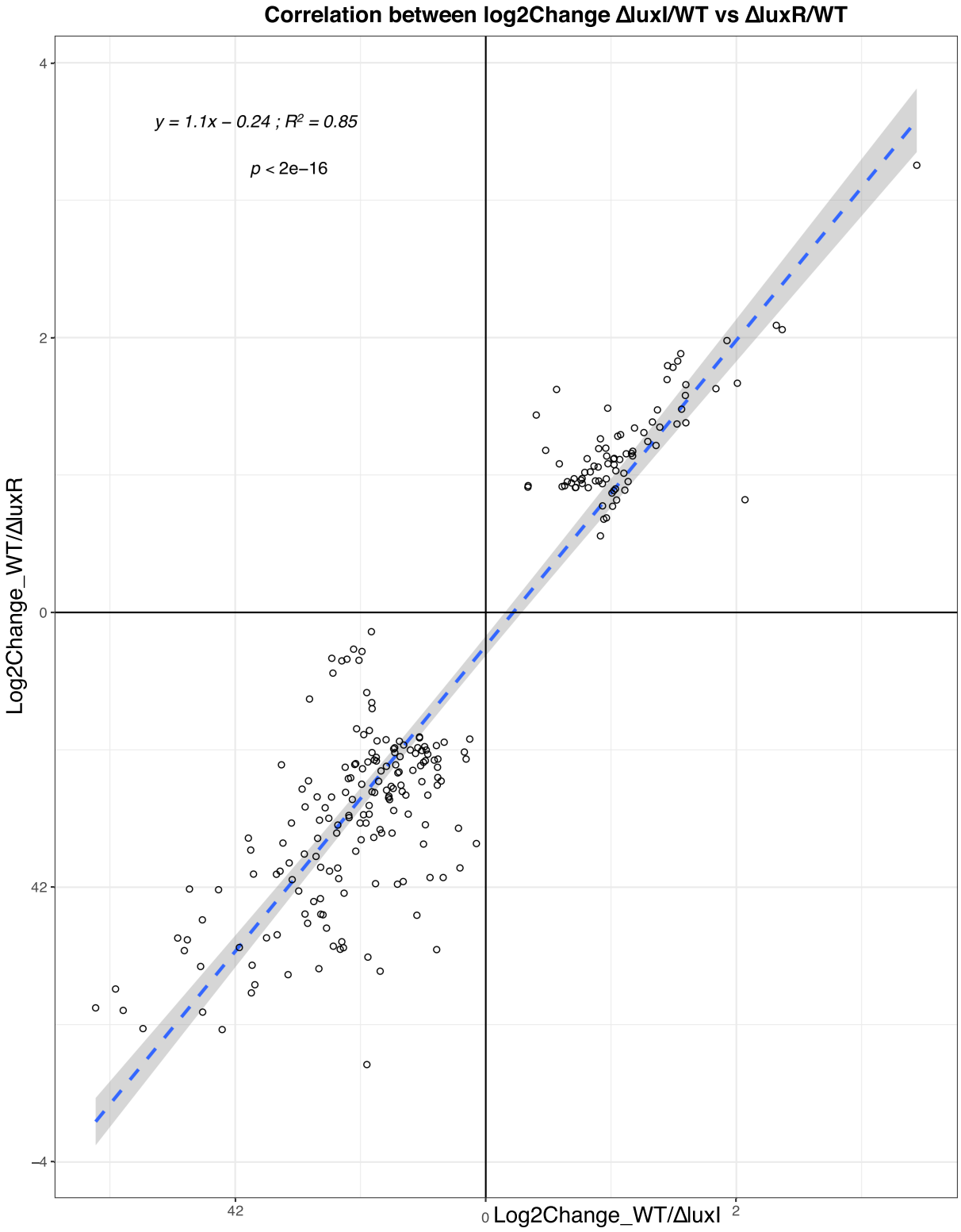

Figure 4. Relationship between the transcriptomic of the Δ*luxI*/WT and Δ*luxR*/WT data comparisons. Linear regression analyses have been done on the log2change data obtained for the two comparisons and the R^2 and *P*-value are presented.

4.1.1.8), and NKI69451.1 encoding an oxalate/formate antiporter. Among these, only the gene NKI69446.1 appeared significantly more expressed in the QS-mutants (log2FC:1.15/2.3). The expression of the gene NKI69443.1 appeared slightly up-regulated, but only in the Δ*colR*/WT treatment comparison and with a negligible log2change value. The second region is composed of 3 genes (NKI67908.1–NKI67910.1) encoding the different subunits (i.e. the b556 cytochrome, the Fe-S small and the large subunits) of a formate dehydrogenase O (EC 1.2.1.2). All of them presented a higher expression (log2FC:1.37–1.87) than in the WT strain.

A total of three distantly related genomic regions involved in glucose metabolism also presented significant upregulation. Indeed, genes encoding a glucose/methanol/choline (GMC) oxidoreductase (EC 1.1.5.9; NKI70795.1, log2FC:1.63; NKI70796.1, log2FC:2.19), a glucokinase (EC 2.7.1.2; NKI70107.1, log2FC:1.49), glucose-6-P DH (NKI70108.1, log2FC:1.75), and a -glutamine: -fructose-6-phosphate aminotransferase (EC 2.6.1.16; NKI71611.1, log2FC:0.98) were also identified.

Several genes related to aminoacid metabolism and peptidoglycan synthesis appeared up-regulated in the QS-mutants. Different genes involved in lysine production and potentially involved in peptidoglycan synthesis [NKI68220.1(EC 1.5.1.7), log2C: 2.46; NKI68260.1 (EC 4.1.1.20), NKI68263.1-NKI68264.1; log2C:1–1.6] presented an increased expression in the QS-mutants. The same was true for genes encoding different enzymes involved in the degradation of leucine [NKI71690.1 (EC 1.4.99.1), log2C:1.12), phenylalanine (NKI71559.1 (EC 1.14.16.1), log2C:3.11], arginine/ornithine [NKI71428.1 (EC 3.5.3.6), log2C:2.38, NKI71429.1 (EC 2.6.1.13), log2C:2.89].

Noticeably, a broad set of genes related to motility ($n = 10$) and belonging to the Type 4 fimbrial assembly system appeared up-regulated in the QS-mutants. These genes presented high sequence homology with *pil* genes (*pilC*, *D*, *M*, *O*, *B*, *P*, and *R*) and the flp/Fap pilin system. Homologues of these genes have been described for their role in synthesis of pili and fimbriae as well as in the twitching mechanism. Several genes of the same genomic regions presented the same trend of expression, but a lower log2change value (*pilA, S, U…*). The single exception was gene NKI70649.1 encoding an homologue of PilT (log2C: −1), which appeared down-regulated in the QS-mutants. PilT possesses an ATPase activity, i.e. essential for the Type IV pili retraction (Burdman et al. 2011).

Noticeably, several genes presenting an up-regulation were predicted by AntiSMASH as members of a cluster identified for strain PMB3(1). Several genes belonging to the NRPS cluster #2 of strain PMB3(1) appeared up-regulated in the QS-mutants. These genes are related to siderophore production, as stated by the recovery of genes encoding the NRPS system (NKI69294.1–NKI69296.1; log2C: −1.23 to −0.91) and the N5-hydroxyornithine formyl transferase (NKI69299.1; log2C: −1.1). All these genes are involved in the production of malleobactin in strain PMB3(1) (Picard et al. 2021). Several genes belonging to the clusters #7/#8 (overlapping clusters) were also detected. These two clusters present homology with a NRPS system involved in rhizomide production or with lipopolysaccharide producing system for cluster #7 and #8, respectively. The genes with an assigned function are NKI69950.1 (non-ribosomal peptide synthetase syringomycin synthetase; log2C = −0.84), NKI69951.1 (Permease, multidrug-efflux transporter, log2C = −1 .45), and NKI69958.1 (5-methyl tetrahydropteroyl triglutamate-homocysteine S-methyltransferase; log2C = −1.62).

Discussion

Sequence characterization of the QS regulatory system of collimonads

Through the combination of genomic, molecular and chemical analyses, we provide the first comprehensive analysis of the QS regulatory system on *Collimonas*. Noticeably, our study identified the *luxIR* homologues (i.e. *colIR*) characterizing strain PMB3(1) and evidenced for the first time the strong sequence conservation of these genes among collimonads whatever their ecological origin and the species considered. Conservation of the *luxIR* sequences and topology is not so common among bacteria, as it is the case for *Agrobacterium* and *Erwinia*. In contrast, representatives of a same species can present very different homologues of *luxI* and *luxR* genes in their genome and strong sequence variation between these genes (e.g. *luxI/luxR* vs. *ainS/R* in *Vibrio fischeri*, *rhlI/rhlR* vs. *lasI/lasR* in *P. aeruginosa*; Gray and Garey 2001, Choudhary et al. 2013).

The conservation observed among *Collimonas* suggests that AHL-based QS regulation represents a key trait in bacteria from this genus. The ability to produce different forms of AHLs varying in their acyl chain length and substitution observed for strain PMB3(1) has also been reported for other rhizosphere bacteria such as *Pseudomonas chlororaphis* and *Pseudomonas fluorescens*, showing that a same AHL synthase can produce different types of AHLs (Shaw et al. 1997, Khan et al. 2005, Peng et al. 2018). The use of UHPLC-MS/MS in our study revealed the dominance in strain PMB3(1), and in most of the *Collimonas* tested, of 3OH- and unsubstituted forms of C6 and C8-HSL, followed by the C10 and C12-HSL. This method also permitted to identify other very low abundance AHLs. This method has already permitted to identify traces of unexpected AHL molecules in well-characterized strains (Ortori et al. 2007, Rasmussen et al. 2014, Patel et al. 2016). As an example, it allowed the identification of six and seven additional AHLs in *E. carotovora* and *P. stewartii* known until recently to only produce 3-oxo-C6-HSL. In our study, the most atypical AHL pattern was observed for strain Ter10, which is characterized by the absence of OH forms of C6 and C8-HSL and very low concentrations of 3OHC10, 3OHC12, 3OC12, and C12-HSL. While this strain presents a functional AHL synthase, as stated by heterologous expression in *E. coli* (i.e. pGEM-T cloning), the *colR* sequence of strain Ter10 presents a stop codon, which may generate a truncated and unfunctional ColR. The pattern observed would correspond to a basal production of AHLs by the AHL synthase at low cell density or in absence of LuxR.

Global view of the QS-regulated genes and similarity between ΔcolR/WT and ΔcolI/WT treatment comparisons

Transcriptomics and proteomics have been applied with success to various species such as *Acinetobacter baumannii*, *Aliivibrio salmonicida*, *P. aeruginosa*, *P. chlororaphis*, *Yersinia pestis*, *Vibrio harveyi*, and various species of *Burkholderia* to decipher the QS regulatory system and the functions regulated (Chugani et al. 2012, Gao et al. 2015, Khider et al. 2019; Ng et al. 2019; Van Kessel et al. 2013). Although the number of *luxIR* systems varies among these model strains, the omics approaches evidenced that 2%–23% of the CDS of *P. aeruginosa*, *Burkholderia thailandensis*, *P. chlororaphis* or *Y. pestis* were regulated in a QS-dependent manner (Arevalo-Ferro et al. 2003, LaRock et al. 2013, Gao et al. 2015, Shah et al. 2020) when comparing the WT strains and their cognate AHL synthase mutant. In strain PMB3(1) that possesses a single AHL synthase, we

observed that only about 3.5% of the genes were regulated in a QS-dependent manner. Although some substantial differences of the expression levels exist between the ΔcolR/WT and ΔcolI/WT treatment comparisons, the significant correlation obtained between the two treatment comparisons demonstrate that the gene regulation were the same between the two QS-mutants. Such correlation and the very low number of genes differentially expressed in the ΔcolI/ΔcolR treatment comparison support the link between *colI* and *colR* as well as the ColR-dependent activation of *colI* in collimonads.

Evidence of metabolic adjustments through a QS regulation

The functional assays performed on the WT strain PMB3(1) and its cognate QS mutants revealed significant variations in carbohydrate, organic acid, and amino acid metabolisms. Most of these variations fit with the transcriptomic responses observed such as the increased growth observed for the QS mutants in presence of glucose (i.e. up-regulation of genes involved in glycolysis and direct oxidative pathways) or formate (i.e. up-regulation of genes involved in formate and oxalate metabolisms). The QS mutants were also characterized by higher Ca-oxalate solubilization ability on solid medium than the WT strain. Oxalate is particularly produced by fungi and has been proposed to act as a signal to guide collimonads to hyphal tips and as a substrate (Rudnick et al. 2015, Haq et al. 2018). In addition, several genes involved in aminio acid (e.g. lysine, leucine, phenylalanine, and arginine/ornithine) degradation or production also appeared differentially expressed in the QS mutants of strain PMB3(1) compared to the WT strain. The functional assays performed revealed a significantly higher leucine aminopeptidase activity in the QS mutants. Although these enzymatic and metabolic changes are not the most commonly described QS-regulated functions, metabolism adjustments have been reported in different studies on pathogens such as *Vibrio cholerae*, *P. aeruginosa*, *Burkholderia glumae*, *A. baumannii*, or *Y. pestis*, and nonpathogen bacteria such *B. thailandensis* or *V. fischeri* (Gao et al. 2015, Davenport et al. 2015, Hawver et al. 2016). The implication of QS in metabolic changes is considered as a physiological adaptation to the niche colonized (Goo et al. 2015). For pathogens or symbionts, the metabolic shift was proposed to be a bypass used by bacteria to shift from the use of the host provided nutrients to the use of derivatives of their own metabolism they accumulate during the first phase of growth. Pyruvate or acetate switches have been reported in various bacteria such as *V. cholera*, *V. fischeri*, or *Y. pestis* (Studer et al. 2008, Hawver et al. 2016). In *V. cholera*, the pyruvate bypass allows the production and the use of acetoin and 2,3-butanediol (Hawver et al. 2016). *Yersinia pestis* switches from the glucose contained in blood to acetate accumulated during the first phase of its development, through the activation of isocitrate lyase and malate synthase (LaRock et al. 2013). In our study, both functional assays and transcriptomics analyses highlighted a preferential metabolism of leucine and formate. Leucine preference was also reported for *A. baumannii* where it was proposed to be an alternative metabolism used by the pathogen (Ng et al. 2019).

Adaptation to nutrient depletion?

Several other functions related to nutrient access appeared differentially regulated in strain PMB3(1) as iron acquisition and phosphate transport. Up-regulation of various genes of the malleobactin NRPS cluster was observed in the QS-mutants, suggesting that this mechanism is activated at low cell density. Regulation of siderophore production through QS dependent mechanism has been evidenced in various taxa, but the production of siderophore can be repressed at low density and activated at high density or *vice versa*, depending on the strain considered (Stintzi et al. 1998, Lewenza et al. 1999). In contrast, phosphate transport appeared down-regulated in the QS-mutants as stated by the differential expression of the phosphate transport systems Pst and Pho. The PhoR/PhoB two-component regulatory system is usually described in P depleted conditions, as an activator of the expression of QS genes (Slater et al. 2003, Krol and Becker 2004). Collimonads are usually recovered from nutrient-poor soils and particularly in the root vicinity, a zone depleted of P and other cations uptaken by the plants. The ecology of collimonads and their effectiveness at solubilizing phosphorus (Uroz et al. 2009) and at mobilizing iron may explain the regulation observed as an nutritional optimization to access limiting nutrients.

QS regulation of motility

Motility is considered as an adaptation process used by bacteria to colonize new surfaces and to disseminate when the nutritive conditions occurring in their local environment are less favourable (Daniels et al. 2004). It is also a phenotype regularly described as QS regulated (Daniels et al. 2004). Mutants impaired in their AHL synthase or in their cognate transcriptional regulator are usually defective for motility, as has been shown in *Aeromonas hydrophila*, *P. aeruginosa*, *Serratia marcescens*, *Sinorhizobium meliloti*, or *V. cholera* (Daniels et al. 2004, Gao et al. 2005). For collimonads, motility has been previously reported as a conserved trait, but without information about the type of mechanisms involved (i.e. swimming, swarming, or twitching) and its regulation (Song et al. 2015). Up-regulation of motility genes in strain Ter331 of *C. fungivorans* was reported during a confrontation assay with *Aspergillus* (Mela et al. 2011), but with no information on a possible density dependent mechanism. Our study represents the first evidence of a relationship between motility and QS as stated by the phenotype of the QS mutants (Fig. 2B). The transcriptome analyses highlight that the motility of collimonads is related to twitching. Indeed, we evidenced a differential expression of several genes involved in the synthesis and functioning of the type IV pili system (i.e. *pilC, D, M, O, B, P, R*, and flp/Fap pilin) in the QS mutants. The T4P system permits colonization of new niches and surface motility (Burdman et al. 2011). In *Vibrio vulnificus*, the Pil system is used to attach on chitin, i.e. considered as an essential reservoir for the survival and persistence of this pathogen (Williams et al. 2015). The link between QS and twitching has already been demonstrated in other taxa as in *A. salmonicida* where a Δ*luxI* mutant is strongly impaired in its motility (Khider et al. 2019). Surprisingly, most of the *pil* genes (*pilC, D, M, O, B, P, R*, and flp/Fap pilin) identified in the genome of strain PMB3(1) appeared up-regulated in the QS-mutants, while these mutants were strongly impaired in their motility as seen in the motility assay. The single exception was the gene *pilT*, which was down-regulated (log2C: -1; NKI70649.1). PilT is considered essential for the T4P retraction due to its ATPase activity. Δ*pilT* mutants are often hyperpiliated and lack pilus retraction and twitching ability (Burdman et al. 2011). Although other regulating factors [e.g. expression stoichiometry of the *pil* genes (Giltner et al. 2012)]; sigma 54 (RpoN) factor (Rendon et al. 2013, Han et al. 2018) can not be excluded, our analyses suggest that the motility of strain PMB3(1) depends on a QS regulation of the ATPase activity of *pilT*.

Conclusions

The integration of the transcriptional responses observed in this study with the functional assays revealed that collimonads reg-

ulate in a QS-dependent way many functions related to environment colonization (i.e. motility), metabolism adjustment (i.e. activation of alternative metabolisms), nutrient access (i.e. siderophore production and phosphate uptake), and microbial interactions (i.e. production of lipo-and thio-peptides). Many of the functions identified in this study have been proposed to play a key role in mycophagy (Leveau and Preston 2008) or have been experimentally evidenced in fungal–bacterial interactions (Mela et al. 2011, Rudnick et al. 2015, Haq et al. 2018). In this sense, differential regulation of genes related to chemotaxis, motility, growth, and EPS production were also reported during confrontation assays between *C. fungivorans* Ter331 and *Aspergillus niger*, suggesting that the QS-regulated functions highlighted in our study may be involved in bacteria–fungi interactions. Our experiments with *L. bicolor* did not reveal a fungal growth inhibition related to QS regulation, but a differential expression of the oxalate metabolism system was observed. Hence, future research will be required to better understand how the QS-dependent regulation system affects *Collimonas*–fungi interactions.

Acknowledgements

The authors thank C. Bach for technical support for the enzymatic assays and the MICROSCOPE team (David Roche; Genoscope) for the support provided on the genome and transcriptome management, Dr. L. Auer for R support and Dr. P. Frey-Klett and W. de Boer for helpful discussions. We thank the Bio2Mar platform and Karine Escoubeyrou for support and access to preparative chemistry and UHPLC-HRMS/MS facilities.

Supplementary data

Supplementary data are available at FEMSEC online.

Conflict of interest statement. None declared.

Funding

This work was supported by grants from the EC2CO program of the CNRS and the Labex ARBRE from the French National Research Agency (ANR) to S.U. The UMR1136 and UR1138 are supported by the ANR through the Labex Arbre (ANR-11-LABX-0002–01).

References

Akum FN, Kumar R, Lai G *et al.* Identification of *Collimonas* gene loci involved in the biosynthesis of a diffusible secondary metabolite with broad-spectrum antifungal activity and plant-protective properties. *Microb Biotechnol* 2021;**14**:1367–84.

An JH, Goo E, Kim H *et al.* Bacterial quorum sensing and metabolic slowing in a cooperative population. *Proc Natl Acad Sci* 2014;**111**:14912–7.

Anders S, Huber W. Differential expression analysis for sequence count data. *Genome Biol* 2010;**11**:R106.

Arevalo-Ferro C, Hentzer M, Reil G *et al.* Identification of quorum-sensing regulated proteins in the opportunistic pathogen *Pseudomonas aeruginosa* by proteomics. *Environ Microbiol* 2003;**5**:1350–69.

Ballhausen MB, Vandamme P, De Boer W. Trait differentiation within the fungus-feeding (mycophagous) bacterial genus *Collimonas*. *PLoS ONE* 2016;**11**:e0157552.

Bonfante P, Anca IA. Plants, mycorrhizal fungi, and bacteria: a network of interactions. *Annu Rev Microbiol* 2009;**63**:363–83.

Brennan CA, Mandel MJ, Gyllborg MC *et al.* Genetic determinants of swimming motility in the squid light-organ symbiont *Vibrio fischeri*. *Microbiologyopen* 2013;**2**:576–94.

Burdman S, Bahar O, Parker JK *et al.* Involvement of type IV pili in pathogenicity of plant pathogenic bacteria. *Genes* 2011;**2**:706–35.

Calvaruso C, Turpault MP, Leclerc E *et al.* Impact of ectomycorrhizosphere on the functional diversity of soil bacterial and fungal communities from a forest stand in relation to nutrient mobilization processes. *Microb Ecol* 2007;**54**:567–77.

Carneiro DG, Almeida FA, Aguilar AP *et al.* *Salmonella enterica* Optimizes metabolism after addition of acyl-homoserine lactone under anaerobic conditions. *Front Microbiol* 2020;**11**:1459.

Chilton M-D, Currier TC, Farrand SK *et al.* *Agrobacterium tumefaciens* DNA and PS8 bacteriophage DNA not detected in crown gall tumors. *Proc Natl Acad Sci* 1974;**71**:3672–6.

Choudhary KS, Hudaiberdiev S, Gelencsér Z *et al.* The organization of the quorum sensing *luxI/R* family genes in *Burkholderia*. *Int J Mol Sci* 2013;**14**:13727–47.

Chugani S, Kim BS, Phattarasukol S *et al.* Strain-dependent diversity in the *Pseudomonas aeruginosa* quorum-sensing regulon. *Proc Natl Acad Sci* 2012;**109**:E2823–31.

Colin Y, Nicolitch O, Turpault MP *et al.* Mineral types and tree species determine the functional and taxonomic structures of forest soil bacterial communities. *Appl Environ Microbiol* 2017;**83**:e02684.

Cretoiu MS, Korthals GW, Visser JH *et al.* Chitin amendment increases soil suppressiveness toward plant pathogens and modulates the actinobacterial and oxalobacteraceal communities in an experimental agricultural field. *Appl Environ Microbiol* 2013;**79**:5291–301.

D'Angelo-Picard C, Faure D, Penot I *et al.* Diversity of N-acyl homoserine lactone-producing and-degrading bacteria in soil and tobacco rhizosphere. *Environ Microbiol* 2005;**7**:1796–808.

Daniels R, Vanderleyden J, Michiels J. Quorum sensing and swarming migration in bacteria. *FEMS Microbiol Rev* 2004;**28**:261–89.

Davenport PW, Griffin JL, Welch M. Quorum sensing is accompanied by global metabolic changes in the opportunistic human pathogen *Pseudomonas aeruginosa*. *J Bacteriol* 2015;**197**:2072–82.

de Boer W, Gunnewiek PJK, Lafeber P *et al.* Anti-fungal properties of chitinolytic dune soil bacteria. *Soil Biol Biochem* 1998;**30**:193–203.

de Boer W, Klein Gunnewiek PJ, Kowalchuk GA *et al.* Growth of chitinolytic dune soil β-subclass Proteobacteria in response to invading fungal hyphae. *Appl Environ Microbiol* 2001;**67**:3358–62.

de Boer W, Leveau JH, Kowalchuk GA *et al.* *Collimonas fungivorans* gen. nov., sp. nov., a chitinolytic soil bacterium with the ability to grow on living fungal hyphae. *Int J Syst Evol Microbiol* 2004;**54**:857–64.

de Boer WD, Folman LB, Summerbell RC *et al.* Living in a fungal world: impact of fungi on soil bacterial niche development. *FEMS Microbiol Rev* 2005;**29**:795–811.

Dennis JJ, Zylstra GJ. Plasposons: modular self-cloning minitransposon derivatives for rapid genetic analysis of Gram-negative bacterial genomes. *Appl Environ Microbiol*. 1998;**64**:2710–5.

DeShazer D, Brett PJ, Carlyon R *et al.* Mutagenesis of *Burkholderia pseudomallei* with Tn5-OT182: isolation of motility mutants and molecular characterization of the flagellin structural gene. *J Bacteriol* 1997;**179**:2116–25.

Deveau A, Palin B, Delaruelle C *et al.* The mycorrhiza helper *Pseudomonas fluorescens* BBc6R8 has a specific priming effect on the growth, morphology and gene expression of the ectomycorrhizal fungus *Laccaria bicolor* S238N. *New Phytol* 2007;**175**:743–55.

Doan HK, Maharaj NN, Kelly KN *et al.* Antimycotal Activity of *Collimonas* isolates and synergy-based biological control of fusarium wilt of tomato. *Phytobiomes J* 2020;**4**:64–74.

Doberva M, Stien D, Sorres J *et al.* Large diversity and original structures of acyl-homoserine lactones in strain MOLA 401, a marine *Rhodobacteraceae* bacterium. *Front Microbiol* 2017;**8**:1152.

El-Gebali S, Mistry J, Bateman A *et al.* The Pfam protein families database in 2019. *Nucleic Acids Res* 2019;**47**:D427–32.

Frey-Klett P, Burlinson P, Deveau A *et al.* Bacterial-fungal interactions: hyphens between agricultural, clinical, environmental, and food microbiologists. *Microbiol Mol Biol Rev* 2011;**75**: 583–609.

Frey-Klett P, Chavatte M, Clausse ML *et al.* Ectomycorrhizal symbiosis affects functional diversity of rhizosphere fluorescent pseudomonads. *New Phytol* 2005;**165**:317–28

Fritsche K, De Boer W, Gerards S *et al.* Identification and characterization of genes underlying chitinolysis in *Collimonas fungivorans* ter331. *FEMS Microbiol Ecol* 2008;**66**:123–35.

Fritsche K, van den Berg M, De Boer W *et al.* Biosynthetic genes and activity spectrum of antifungal polyynes from *Collimonas fungivorans* ter331. *Environ Microbiol* 2014;**16**:1334–45.

Fuqua C, Parsek MR, Greenberg EP. Regulation of gene expression by cell-to-cell communication: acyl-homoserine lactone quorum sensing. *Annu Rev Genet* 2001;**35**:439–68.

Fuqua WC, Winans SC, Greenberg EP. Quorum sensing in bacteria: the LuxR-LuxI family of cell density-responsive transcriptional regulators. *J Bacteriol* 1994;**176**:269.

Gao M, Chen H, Eberhard A *et al.* sinI-and expR-dependent quorum sensing in *Sinorhizobium meliloti*. *J Bacteriol* 2005;**187**:7931–44.

Gao R, Krysciak D, Petersen K *et al.* Genome-wide RNA sequencing analysis of quorum sensing-controlled regulons in the plant-associated *Burkholderia glumae* PG1 strain. *Appl Environ Microbiol* 2015;**81**:7993–8007.

Giltner CL, Nguyen Y, Burrows LL. Type IV pilin proteins: versatile molecular modules. *Microbiol Mol Biol Rev* 2012;**76**:740–72.

González I, Lê Cao KA, Davis MJ *et al.* Visualising associations between paired 'omics' data sets. *BioData Mining* 2012;**5**:19.

Goo E, An JH, Kang Y *et al.* Control of bacterial metabolism by quorum sensing. *Trends Microbiol* 2015;**23**:567–76.

Gouy M, Guindon S, Gascuel O. SeaView version 4: a multiplatform graphical user interface for sequence alignment and phylogenetic tree building. *Mol Biol Evol* 2010;**27**:221–4.

Gray KM, Garey JR The evolution of bacterial LuxI and LuxR quorum sensing regulators. *Microbiology* 2001;**147**:2379–87.

Haack FS, Poehlein A, Kröger C *et al.* Molecular keys to the *Janthinobacterium* and *duganella* spp. interaction with the plant pathogen *Fusarium graminearum*. *Front Microbiol* 2016;**7**:1668.

Han S, Shen D, Zhao Y *et al.* Sigma factor RpoN employs a dual transcriptional regulation for controlling twitching motility and biofilm formation in lysobacter enzymogenes OH11. *Curr Genet* 2018;**64**:515–27.

Haq IU, Zwahlen RD, Yang P *et al.* The response of *Paraburkholderia terrae* strains to two soil fungi and the potential role of oxalate. *Front Microbiol* 2018;**9**:989.

Hawver LA, Giulietti JM, Baleja JD *et al.* Quorum sensing coordinates cooperative expression of pyruvate metabolism genes to maintain a sustainable environment for population stability. *MBio* 2016;**7**:e01863–16.

Höppener-Ogawa S, de Boer W, Leveau JHJ *et al. Collimonas arenae* sp. nov. and *Collimonas pratensis* sp. nov., isolated from (semi-) natural grassland soils. *Int J Syst Evol Microbiol* 2008;**58**:414–9.

Johansson JF, Paul LR, Finlay RD. Microbial interactions in the mycorrhizosphere and their significance for sustainable agriculture. *FEMS Microbiol Ecol* 2004;**48**:1–13.

Kamilova F, Leveau JH, Lugtenberg B. *Collimonas fungivorans*, an unpredicted in vitro but efficient in vivo biocontrol agent for the suppression of tomato foot and root rot. *Environ Microbiol* 2007;**9**:1597–603.

Khan SR, Mavrodi DV, Jog GJ *et al.* Activation of the *phz* operon of *Pseudomonas fluorescens* 2-79 requires the LuxR homolog PhzR, N-(3-OH-hexanoyl)-L-homoserine lactone produced by the LuxI homolog PhzI, and a cis-acting phz box. *J Bacteriol* 2005;**187**:6517–27.

Khider M, Hansen H, Hjerde E *et al.* Exploring the transcriptome of luxI– and ΔainS mutants and the impact of N-3-oxo-hexanoyl-L-and N-3-hydroxy-decanoyl-L-homoserine lactones on biofilm formation in *Aliivibrio salmonicida*. *PeerJ* 2019;**7**:e6845.

Kleerebezem M, Quadri LE, Kuipers OP *et al.* Quorum sensing by peptide pheromones and two-component signal-transduction systems in Gram-positive bacteria. *Mol Microbiol* 1997;**24**:895–904.

Kovach ME, Elzer PH, Hill DS *et al.* Four new derivatives of the broad-host-range cloning vector pBBR1MCS, carrying different antibiotic-resistance cassettes. *Gene* 1995;**166**:175–6.

Krol E, Becker A. Global transcriptional analysis of the phosphate starvation response in *Sinorhizobium meliloti* strains 1021 and 2011. *Mol Genet Genomics* 2004;**272**:1–17.

LaRock CN, Yu J, Horswill AR *et al.* Transcriptome analysis of acetyl-homoserine lactone-based quorum sensing regulation in *Yersinia pestis*. *PLoS ONE* 2013;**8**:e62337.

Lee SD. *Collimonas antrihumi* sp. nov., isolated from a natural cave and emended description of the genus *Collimonas*. *Int J Syst Evol Microbiol* 2018;**68**:2448–53.

Lepleux C, Turpault MP, Oger P *et al.* Correlation of the abundance of betaproteobacteria on mineral surfaces with mineral weathering in forest soils. *Appl Environ Microbiol* 2012;**78**:7114–9.

Leveau JH, Preston GM. Bacterial mycophagy: definition and diagnosis of a unique bacterial–fungal interaction. *New Phytol* 2008;**177**:859–76.

Leveau JH, Uroz S, De Boer W. The bacterial genus *Collimonas*: mycophagy, weathering and other adaptive solutions to life in oligotrophic soil environments. *Environ Microbiol* 2010;**12**:281–92.

Lewenza S, Conway B, Greenberg EP *et al.* Quorum sensing in *Burkholderia cepacia*: identification of the LuxRI homologs CepRI. *J Bacteriol* 1999;**181**:748–56.

Li H, Durbin R. Fast and accurate short read alignment with burrows–wheeler transform. *Bioinformatics* 2009;**25**:1754–60.

Li J, Pan M, Zhang X *et al. Collimonas silvisoli* sp. nov. and *Collimonas humicola* sp. nov., two novel species isolated from forest soil. *Int J Syst Evol Microbiol* 2021;**71**:005061.

Love MI, Huber W, Anders S. Moderated estimation of fold change and dispersion for RNA-seq data with DESeq2. *Genome Biol* 2014;**15**:550.

Luo ZQ, Su S, Farrand SK. In situ activation of the quorum-sensing transcription factor TraR by cognate and noncognate acyl-homoserine lactone ligands: kinetics and consequences. *J Bacteriol* 2003;**185**:5665–72.

Männistö MK, Häggblom MM. Characterization of psychrotolerant heterotrophic bacteria from Finnish lapland. *Syst Appl Microbiol* 2006;**29**:229–43.

Marupakula S, Mahmood S, Jernberg J *et al.* Bacterial microbiomes of individual ectomycorrhizal *Pinus sylvestris* roots are shaped by soil horizon and differentially sensitive to nitrogen addition. *Environ Microbiol* 2017;**19**:4736–53.

McClean KH, Winson MK, Fish L *et al.* Quorum sensing and *Chromobacterium violaceum*: exploitation of violacein production and inhibition for the detection of N-acylhomoserine lactones. *Microbiology* 1997;**143**:3703–11.

Mela F, Fritsche K, De Boer W *et al.* Dual transcriptional profiling of a bacterial/fungal confrontation: *Collimonas fungivorans* versus *Aspergillus niger*. *ISME J* 2011;**5**:1494–504.

Mukherjee S, Bassler BL. Bacterial quorum sensing in complex and dynamically changing environments. *Nat Rev Microbiol* 2019;**17**:371–82.

Ng CK, How KY, Tee KK *et al.* Characterization and transcriptome studies of autoinducer synthase gene from multidrug resistant *Acinetobacter baumannii* strain 863. *Genes* 2019;**10**:282.

Ortori CA, Atkinson S, Chhabra SR *et al.* Comprehensive profiling of N-acylhomoserine lactones produced by *Yersinia pseudotuberculosis* using liquid chromatography coupled to hybrid quadrupole–linear ion trap mass spectrometry. *Anal BioanalChem* 2007;**387**:497–511.

Palla M, Battini F, Cristani C *et al.* Quorum sensing in rhizobia isolated from the spores of the mycorrhizal symbiont *Rhizophagus intraradices*. *Mycorrhiza* 2018;**28**:773–8.

Papenfort K, Bassler BL. Quorum sensing signal–response systems in Gram-negative bacteria. *Nat Rev Microbiol* 2016;**14**:576.

Parks DH, Imelfort M, Skennerton CT *et al.* CheckM: assessing the quality of microbial genomes recovered from isolates, single cells, and metagenomes. *Genome Res* 2015;**25**:1043–55.

Patel NM, Moore J D, Blackwell HE *et al.* Identification of unanticipated and novel N-acyl L-homoserine lactones (AHLs) using a sensitive non-targeted LC-MS/MS method. *PLoS ONE* 2016;**11**:e0163469.

Peng H, Ouyang Y, Bilal M *et al.* Identification, synthesis and regulatory function of the N-acylated homoserine lactone signals produced by *Pseudomonas chlororaphis* HT66. *Microb Cell Fact* 2018;**17**:1–11.

Picard L, Oger P, Turpault MP *et al.* Draft Genome Sequence of Collimonas pratensis Strain PMB3, an Effective Mineral-Weathering and Chitin-Hydrolyzing Bacterial Strain. *Microbiology Resource Announcements* 2020;**9**:e00601–20.

Picard L, Paris C, Dhalleine T *et al.* The mineral weathering ability of *Collimonas pratensis* PMB3 (1) involves a malleobactin-mediated iron acquisition system. *Environ Microbiol* 2021;**22**:3838–62.

Pierson III LS, Pierson EA. Phenazine antibiotic production in *Pseudomonas aureofaciens*: role in rhizosphere ecology and pathogen suppression. *FEMS Microbiol Lett* 1996;**136**:101–8.

Pospiech A, Neumann B. A versatile quick-prep of genomic DNA from Gram-positive bacteria. *Trends Genet* 1995;**11**:217–8.

Pratama AA, van Elsas JD. Gene mobility in microbiomes of the mycosphere and mycorrhizosphere–role of plasmids and bacteriophages. *FEMS Microbiol Ecol* 2019;**95**:fiz053.

Rambelli A. The rhizosphere of mycorrhizae. In: *Ectomycorrhizae: Their Ecology and Physiology*. Cambridge: Academic Press, 1973, 299–343.

Rankl S, Gunsé B, Sieper T *et al.* Microbial homoserine lactones (AHLs) are effectors of root morphological changes in barley. *Plant Sci* 2016;**253**:130–40.

Rasmussen BB, Nielsen KF, Machado H *et al.* Global and phylogenetic distribution of quorum sensing signals, acyl homoserine lactones, in the family of *Vibrionaceae*. *Mar Drugs* 2014;**12**:5527–46.

Rasmussen TB, Skindersoe ME, Bjarnsholt T *et al.* Identity and effects of quorum-sensing inhibitors produced by *Penicillium* species. *Microbiology* 2005;**151**:1325–40.

Rendón MA, Hockenberry AM, McManus SA *et al.* Sigma factor RpoN (σ54) regulates pilE transcription in commensal *Neisseria elongata*. *Mol Microbiol* 2013;**90**:103–13.

Rodrigues AM, Lami R, Escoubeyrou K *et al.* Straightforward N-Acyl homoserine lactone discovery and annotation by LC–MS/MS-based molecular networking. *J Proteome Res* 2022;**21**:635–42.

Rohart F, Gautier B, Singh A *et al.* mixOmics: an R package for 'omics feature selection and multiple data integration. *PLoS Comput Biol* 2017;**13**:e1005752.

Romani M, Adouane E, Carrion C *et al.* Diversity and activities of pioneer bacteria, algae, and fungi colonizing ceramic roof tiles during the first year of outdoor exposure. *Int Biodeterior Biodegrad* 2021;**162**:105230.

Romero M, Avendaño-Herrera R, Magariños B *et al.* Acylhomoserine lactone production and degradation by the fish pathogen *Tenacibaculum maritimum*, a member of the *Cytophaga–Flavobacterium–Bacteroides* (CFB) group. *FEMS Microbiol Lett* 2010;**304**:131–9.

Rudnick MB, Van Veen JA, De Boer W. Oxalic acid: a signal molecule for fungus-feeding bacteria of the genus *Collimonas*?. *Environ Microbiol Rep* 2015;**7**:709–14.

Schaefer AL, Lappala CR, Morlen RP *et al.* LuxR-and LuxI-type quorum-sensing circuits are prevalent in members of the *Populus deltoides* microbiome. *Appl Environ Microbiol* 2013;**79**:5745–52.

Schäfer A, Tauch A, Jäger W *et al.* Small mobilizable multi-purpose cloning vectors derived from the *Escherichia coli* plasmids pK18 and pK19: selection of defined deletions in the chromosome of *Corynebacterium glutamicum*. *Gene* 1994;**145**:69–73.

Schwyn B, Neilands JB. Universal chemical assay for the detection and determination of siderophores. *Anal Biochem* 1987;**160**:47–56.

Senechkin IV, van Overbeek LS, Er HL *et al.* Interaction of *Collimonas* strain IS343 with *Rhizoctonia solani* at low carbon availability in vitro and in soil. *Eur J Plant Pathol* 2013;**136**:789–802.

Shah N, Gislason AS, Becker M *et al.* Investigation of the quorum-sensing regulon of the biocontrol bacterium *Pseudomonas chlororaphis* strain PA23. *PLoS ONE* 2020;**15**:e0226232.

Shaw PD, Ping G, Daly SL *et al.* Detecting and characterizing N-acylhomoserine lactone signal molecules by thin-layer chromatography. *Proc Natl Acad Sci* 1997;**94**:6036–41.

Slater H, Crow M, Everson L *et al.* Phosphate availability regulates biosynthesis of two antibiotics, prodigiosin and carbapenem, in *Serratia* via both quorum-sensing-dependent and -independent pathways. *Mol Microbiol* 2003;**47**:303–20. https://doi.org/10.1046/j.1365-2958.2003.03295.x

Song C, Schmidt R, de Jager V *et al.* Exploring the genomic traits of fungus-feeding bacterial genus *Collimonas*. *BMC Genomics* 2015;**16**:1103.

Sperandio V. SdiA sensing of acyl-homoserine lactones by enterohemorrhagic *e. coli* (EHEC) serotype O157:H7 in the bovine rumen. *Gut Microbes* 2010;**1**:432–5

Steidle A, Sigl K, Schuhegger R *et al.* Visualization of N-acylhomoserine lactone-mediated cell-cell communication between bacteria colonizing the tomato rhizosphere. *Appl Environ Microbiol* 2001;**67**:5761–70.

Steindler L, Venturi V. Detection of quorum-sensing N-acyl homoserine lactone signal molecules by bacterial biosensors. *FEMS Microbiol Lett* 2007;**266**:1–9.

Stintzi A, Evans K, Meyer JM *et al.* Quorum-sensing and siderophore biosynthesis in *Pseudomonas aeruginosa*: lasRllasI mutants exhibit reduced pyoverdine biosynthesis. *FEMS Microbiol Lett* 1998;**166**:341–5.

Studer SV, Mandel MJ, Ruby EG. AinS quorum sensing regulates the *Vibrio fischeri* acetate switch. *J Bacteriol* 2008;**190**:5915–23.

Swift S, Downie JA, Whitehead NA *et al.* Quorum sensing as a population-density-dependent determinant of bacterial physiology. *Adv Microb Physiol* 2001;**45**:199–270.

Tichi MA, Tabita FR. Metabolic signals that lead to control of cbb gene expression in rhodobacter capsulatus. *J Bacteriol* 2002;**184**:1905–15.

Turnbull L, Whitchurch CB. Motility assay: twitching motility. In: *Pseudomonas Methods and Protocols*. New York: Humana Press, 2014, 73–86.

Uroz S, Calvaruso C, Turpault MP *et al.* Effect of the mycorrhizosphere on the genotypic and metabolic diversity of the bacterial communities involved in mineral weathering in a forest soil. *Appl and environ microbiol* 2007;**73**:3019–27.

Uroz S, Calvaruso C, Turpault MP *et al.* Mineral weathering by bacteria: ecology, actors and mechanisms. *Trends in microbiology* 2009;**17**:378–87.

Uroz S, Courty PE, Oger P. Plant symbionts are engineers of the plant-associated microbiome. *Trends Plant Sci* 2019;**24**:905–16.

Uroz S, Courty PE, Pierrat JC *et al.* Functional profiling and distribution of the forest soil bacterial communities along the soil mycorrhizosphere continuum. *Microb Ecol* 2013;**66**:404–15.

Uroz S, D'Angelo-Picard C, Carlier A *et al.* Novel bacteria degrading N-acylhomoserine lactones and their use as quenchers of quorum-sensing-regulated functions of plant-pathogenic bacteria. *Microbiology* 2003;**149**:1981–9.

Uroz S, Heinonsalo J. Degradation of N-acyl homoserine lactone quorum sensing signal molecules by forest root-associated fungi. *FEMS Microbiol Ecol* 2008;**65**:271–8.

Uroz S, Oger P, Morin E *et al.* Distinct ectomycorrhizospheres share similar bacterial communities as revealed by pyrosequencing-based analysis of 16S rRNA genes. *Appl Environ Microbiol* 2012;**78**:3020–4.

Uroz S, Tech JJ, Sawaya NA *et al.* Structure and function of bacterial communities in ageing soils: insights from the mendocino ecological staircase. *Soil Biol Biochem* 2014;**69**:265–74.

Vallenet D, Calteau A, Mathieu Dubois M *et al.* MicroScope: an integrated platform for the annotation and exploration of microbial gene functions through genomic, pangenomic and metabolic comparative analysis. *Nucleic Acids Res* 2019;**48**:D579–89.

Van Kessel JC, Ulrich LE, Zhulin IB *et al.* Analysis of activator and repressor functions reveals the requirements for transcriptional control by LuxR, the master regulator of quorum sensing in *Vibrio harveyi*. *MBio* 2013;**4**:e00378–13.

Venturi V, Keel C. Signaling in the rhizosphere. *Trends Plant Sci* 2016;**21**:187–98.

Viollet A, Corberand T, Mougel C *et al.* Fluorescent pseudomonads harboring type III secretion genes are enriched in the mycorrhizosphere of *Medicago truncatula*. *FEMS Microbiol Ecol* 2011;**75**:457–67.

Whitehead NA, Barnard AM, Slater H *et al.* Quorum-sensing in Gram-negative bacteria. *FEMS Microbiol Rev* 2001;**25**:365–404.

Whitehead NA, Byers JT, Commander P *et al.* The regulation of virulence in phytopathogenic *Erwinia* species: quorum sensing, antibiotics and ecological considerations. *Antonie Van Leeuwenhoek* 2002;**81**:223–31.

Williams TC, Ayrapetyan M, Oliver JD. Molecular and physical factors that influence attachment of *Vibrio vulnificus* to chitin. *Appl Environ Microbiol* 2015;**81**:6158–65.

Winson MK, Camara M, Latifi A *et al.* Multiple N-acyl-L-homoserine lactone signal molecules regulate production of virulence determinants and secondary metabolites in *Pseudomonas aeruginosa*. *Proc Natl Acad Sci* 1995;**92**:9427–31.

Wisniewski-Dyé F, Downie JA. Quorum-sensing in *Rhizobium*. *Antonie Van Leeuwenhoek* 2002;**81**:397–407.

Wood DW, Gong F, Daykin MM *et al.* N-acyl-homoserine lactone-mediated regulation of phenazine gene expression by *Pseudomonas aureofaciens* 30-84 in the wheat rhizosphere. *J Bacteriol* 1997;**179**:7663–70.

Zúñiga A, Poupin MJ, Donoso R *et al.* Quorum sensing and indole-3-acetic acid degradation play a role in colonization and plant growth promotion of *Arabidopsis thaliana* by *Burkholderia phytofirmans* PsJN. *Mol Plant Microbe Interact* 2013;**26**:546–53.